Chapter 5

Synthesis and study of indoloquinoxaline based D-π-A molecules and their application as fluorescent probe for hypochlorite detection

Table of contents

Introduction

Donor-π-acceptor (D-π-A) conjugated molecules are important materials in optoelectronics and have gained significant attention in recent years due to their unique electronic properties and potential applications.[1] These molecules are designed to have a specific molecular structure consisting of three main components: an electron-donating group (D), a π-spacer, and an electron-accepting group (A). This design facilitates intramolecular charge transfer (ICT) and leads to a variety of interesting spectroscopic and optoelectronic features. The donor is typically a group or moiety within the molecule that has a relatively higher electron density or is capable of donating electrons. Common D groups include electron-rich aromatic rings or heterocycles with lone pair electrons.[2,3] The presence of D helps in the initial absorption of light energy and facilitates the generation of excited electronic states. The π-spacer is a conjugated bridge or linker between the D and A groups. It consists of alternating single and multiple bonds, often containing conjugated double bonds (π electrons). The π-spacer plays a crucial role in mediating the electronic coupling between the D and A groups. It allows for efficient electronic communication between these groups, enabling the ICT process. The A component is typically a group or moiety within the molecule that has a relatively lower electron density or is electron-deficient.[4] Common A groups include electron-poor aromatic rings, such as nitro or cyno groups.[5,6]

The spectroscopic features of D-π-A molecules are closely associated with ICT excitations, where electrons are transferred from the D to A moiety upon absorbing light. This leads to several important characteristics.[7] D-π-A molecules often exhibit absorption spectra with longer-wavelength peaks compared to their individual D and A components. This red-shift in absorption is indicative of efficient ICT. The ICT process can lead to an increase in fluorescence emission, making D-π-A molecules useful in applications like fluorescence-based sensors and organic light-emitting diodes (OLEDs).[8]

Due to their ICT effects and tuneable optical properties, D-π-A-based conjugated molecules find applications in organic photovoltaics, organic semiconductors, organic light-emitting devices (OLEDs), and molecular sensors. They offer opportunities for efficient charge transport and energy conversion, making them essential materials in the development of next-generation optoelectronic technologies.

D-π-A based conjugated molecules have been widely applied in fluorescence imaging, organic light emitting diodes,[9–12] dye-sensitized solar cells, [13–15] sensors,[16,17] transistors,[18,19] and nonlinear optical technologies.[20]

D-π-A molecules are a class of conjugated organic compounds that have a specific molecular structure designed for certain optical and electronic properties. D-π-A molecules are known for their strong solvatochromism effects.[21] Solvatochromism refers to the phenomenon where the absorption and emission wavelengths of a molecule change depending on the polarity of the solvent. The absorption and emission spectra of D-π-A molecules can vary due to variations in solvent polarity. [22] The structure of D-π-A molecules has a significant influence on their fluorescence properties. By carefully designing the D-π-A energy level structure of these molecules, researchers can control their fluorescent properties.[23]

D-π-A molecules have been utilized as fluorescent probes in various applications due to their high sensitivity, specificity, and high spatiotemporal resolution. This makes them valuable tools in various fields, such as chemistry, biology, and materials science.[24] Due to their solvatochromism effects D-π-A molecules are used as fluorescent probes in various applications. Their design, including the energy level structure and choice of spacer or anchor groups, is crucial in tailoring their fluorescence properties for specific purposes. These molecules are valued for their sensitivity and specificity in detecting various ions/substances and their ability to provide high spatiotemporal resolution in imaging and sensing applications.[25,26]

D-π-A molecules, are a class of organic compounds commonly used in organic electronics and photovoltaic devices. These molecules are designed to have specific electronic and optical properties that make them suitable for various applications, such as organic solar cells and organic light-emitting diodes (OLEDs). The electronic and optical properties of D-π-A molecules can be fine-tuned through chemical modifications of the donor, π-spacer, and acceptor groups. Changing the donor group can significantly impact on the electronic properties.[27] A stronger donor group can increase the electron-donating ability, leading to a lower lowest unoccupied molecular orbital (LUMO) energy level and a narrower bandgap. Modifying the donor group can alter the electron density on the donor moiety, which in turn, affects the charge transfer efficiency between the donor and acceptor units.[28]

The length of the π-spacer can influence the distance between the donor and acceptor units. A longer π-spacer can decrease electronic coupling between these groups, affecting charge transfer rates.[29] The degree of conjugation in the π-spacer can also be adjusted. Enhanced conjugation can lower the highest occupied molecular orbital (HOMO) energy level and broaden the absorption spectrum.[30] Altering the acceptor group can affect the electron-accepting ability of the molecule. A stronger acceptor group can lead to a lower HOMO energy level and a broader absorption spectrum. Introduction of electron-withdrawing groups on the acceptor unit can further increase its electron-accepting ability and decrease the HOMO energy level. Increasing the conjugation length across the entire D-π-A molecule can also impact the electronic and optical properties.[31] Longer conjugation often results in a broader absorption spectrum and more efficient charge transport. The steric hindrance caused by bulky substituents on the molecule can affect the molecular packing in solid-state devices, potentially influencing charge mobility and device performance.[32]

6*H*-Indolo[2,3-*b*]quinoxaline is a compound with a fused electron-rich indole and electron-deficient quinoxaline moieties (Figure 5.1).[33] This arrangement has several benefits, including dipolar structure, Its better intramolecular charge transfer and Extended π-conjugation is possible because to the coplanar structure. [34] It has the ability to form π-stacked aggregates both in solution and in the solid state due to strong π-π interactions.[35]

6*H*-Indolo[2,3-*b*]quinoxaline has been used as an electron-transporting and emitting layer in organic light emitting diodes (OLEDs).[36] It serves as organic sensitizers for dye-sensitized solar cells (DSSCs).[37] It is used as hole-injection materials in multi-layered OLEDs. The compound has been incorporated into a conjugated polymer, resulting in a polymer with very high space charge limited current (SCLC) hole mobility.[38] A single crystal X-ray diffraction study of the indoloquinoxaline-based compound revealed strong π···π interactions and a high planar framework.[33,39]

6*H*-Indolo[2,3-*b*]quinoxaline is a versatile compound with unique properties, making it valuable for various applications in the field of organic electronics, including OLEDs, solar cells. Its ability to form strong π-π interactions and its extended π-conjugation are key factors contributing to its utility in these applications.[27,40]

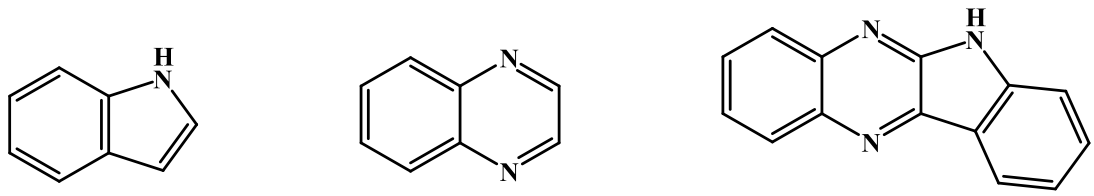

indole **quinoxaline** **6H-indolo[2,3-b]quinoxaline**

Figure 5.1 Structures of indole, quinoxaline and 6*H*-indolo[2,3-*b*]quinoxaline.

A new class of 6*H*-indolo[2,3-*b*]quinoxaline derivatives, a novel class of organic dyes are synthesised by Qian *et al*.[27] and they are used as photosensitizers for dye-sensitized solar cells. The dyes **JY01**, **JY02**, and **JY03** are synthesized by introducing several electron-rich *p*-conjugated bridges, such as oligothiophene, thienyl carbazole, and furyl carbazole (Figure 5.2) Which are coupled with the anchoring group of cyanoacrylic acid and 6H-indolo[2,3-b] quinoxaline. Their photovoltaic, electrochemical, and photophysical characteristics are being studied further. All three dyes have strong photosensitizing abilities. With a short-circuit photocurrent density of 16.0 mA cm^2, an open-circuit photovoltage of 708 mV, and a fill factor of 0.67, the DSSC based on **JY01** exhibits the best photovoltaic performance, translating to an overall power conversion efficiency of 7.62% under AM 1.5 irradiation (100 mW cm^2).

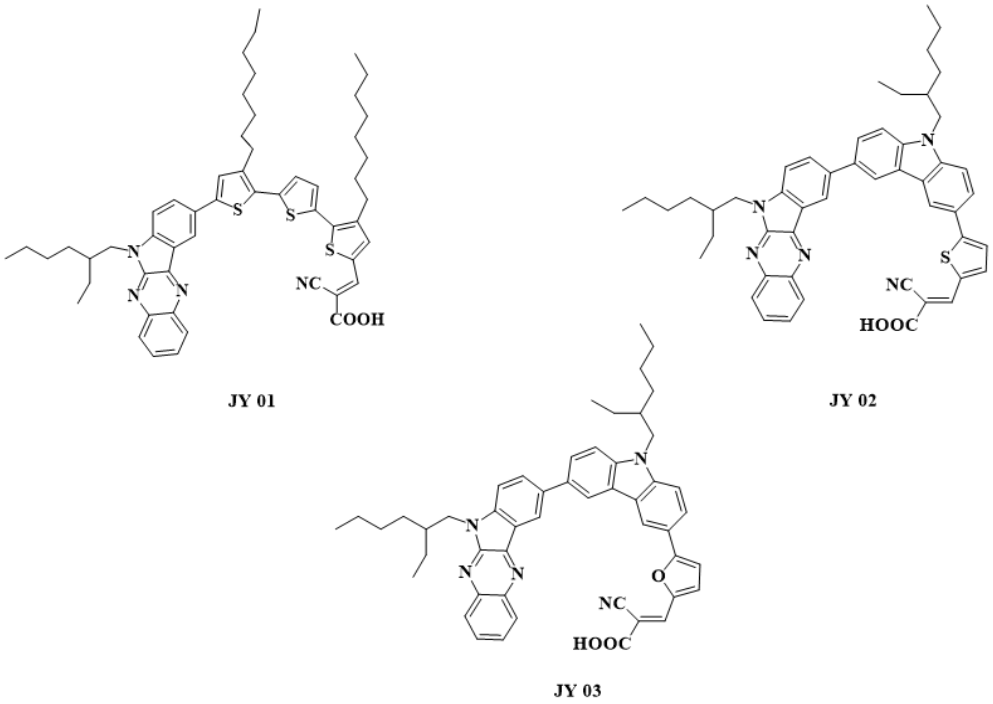

Figure 5.2 Structures of the dyes **JY01**, **JY02**, and **JY03** [27]

All dyes contain an indoloquinoxaline core and a 2- cyanoacrylic acid group which acts as the electron donor and the electron acceptor groups, respectively. Different electron-rich conjugated linkers such as oligothiophene (**JY 01**), thienyl carbazole (**JY 02**), and furyl carbazole (**JY 03**) were use as the π-bridges. Due to its superior electron delocalization throughout the whole molecule, an electron-rich π-conjugated linker is preferred to induce effective ICT to low energy solar photons

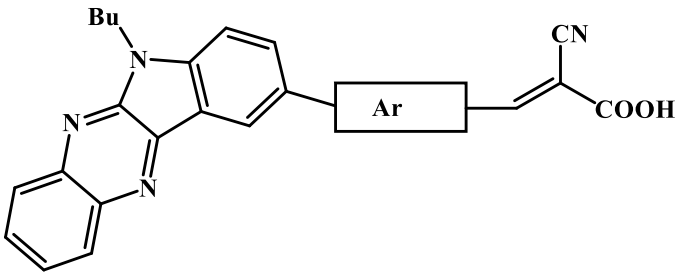

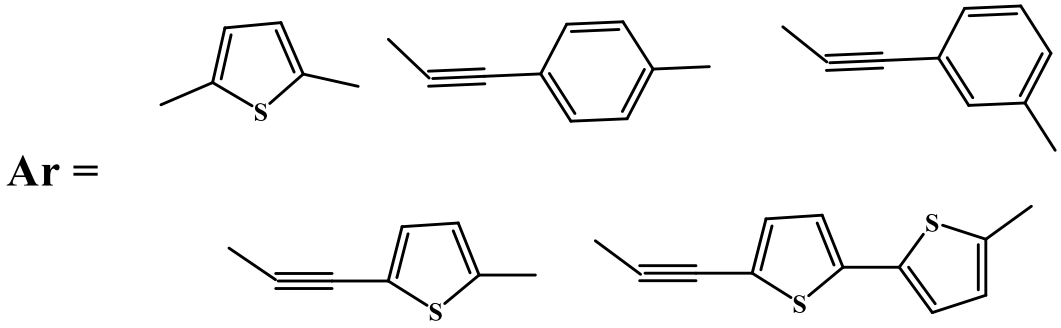

Figure 5.3 Structures of the indoloquinoxaline-based dyes [41]

Different linkers between donor (D) and acceptor (A) fragments in D-A organic dye have been investigated by Venkateswararao *et al.*[41] utilising the fragments of triarylamine and cyanoacrylic acid as the donor and acceptor units, respectively. Due to the localised π-π* transitions in the 300–500 nm range, all dyes showed numerous peaks. Absorption peaks for indolo[3,2-*b*]quinoxaline may be found at wavelengths of 290 nm, 330 nm, 355 nm, and 420 nm. The charge transfers from the indole to quinoxaline segment causes the longer wavelength absorption (420 nm), whereas the lower wavelength bands are caused by the π-π* and n-π* transitions. Among all dyes, a dye containing thiophene in the *p*-spacer exhibited the highest device efficiency.

A simple chemosensor that successfully detected hypochlorite and hydrazine with outstanding performance was created by condensation of 7-diethylaminocoumarin with barbituric acid was synthesised by Wu *et al.*[42]

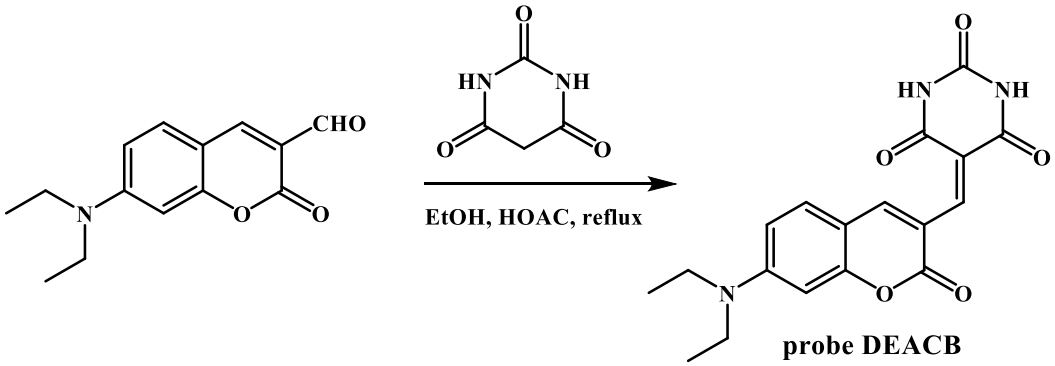

Figure 5.4 Synthesis of chemosensor DEACB [42]

Wu *et al.*[42] synthesised a coumarin-based chemosensor that demonstrated outstanding dual-mode detection capabilities for sensing ClO^- and N_2H_4 based on several reaction processes. This chemosensor demonstrated a clear alteration in the UV

absorption spectra in DMSO/PBS(phosphate buffered saline)(9/1, v/v) solution and showed quenching of fluorescence upon addition of ClO^-. Interestingly, when it was developed as a practical test paper, it displayed turn-on fluorescence response to ClO^-. In contrast, the chemosensor significantly increased its fluorescence in DMSO/PBS (1/9, v/v) solution after reacting with N_2H_4. Additionally, it was able to scan N_2H_4 in living cells with minimal cytotoxicity. Wu *et al*. synthesised a straightforward chemosensor by condensation of 7-diethylaminocoumarin with barbituric acid, which reliably and exceptionally well detected hypochlorite and hydrazine.

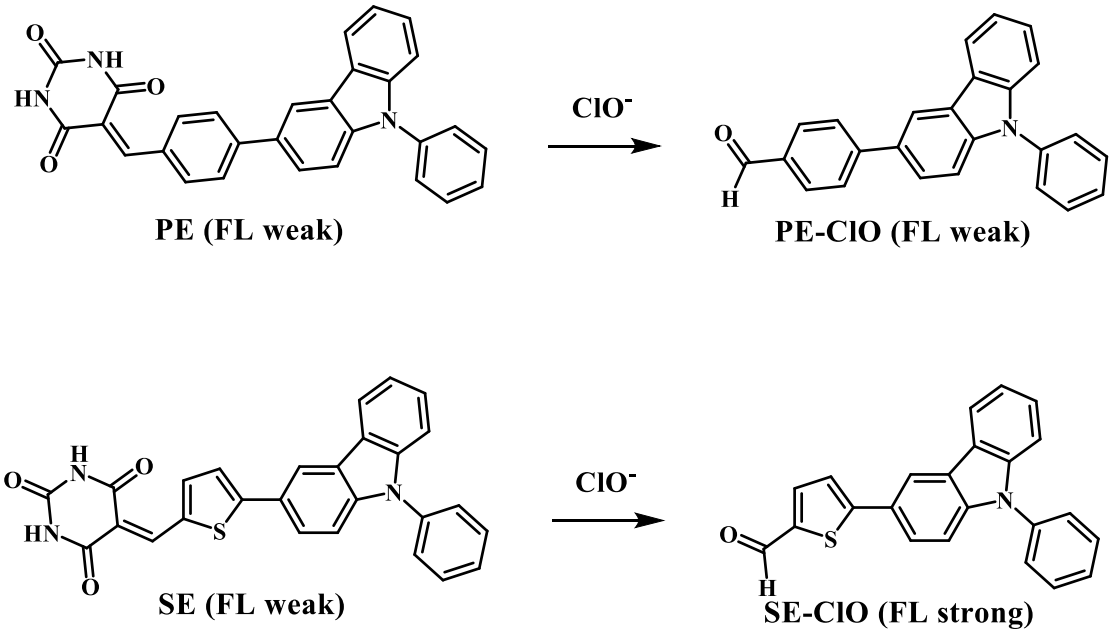

Figure 5.5 Schematic illustration of sensing mechanism of PE and SE towards ClO^-.[4]

Two unique D-π-A and ICT type compounds (SE and PE) are synthesised by Wu *et al.*[4] by altering the conjugation bridge, in order to investigate the use of D-π-A molecules in bio-imaging. The carbazole and pyrimidine units have a high intramolecular charge transfer (ICT) effect, which causes SE and PE to emit only weak fluorescence in an aqueous solution. It's interesting to note that SE exhibits improved fluorescence detection capabilities for hypochlorite due to the D-π-A structure and appropriate ICT effect following the oxidative cleavage of the alkene unit by hypochlorite. It's significant that the cell membrane permeable SE can be used for both exogenous and endogenous ClO^- in living cells and zebrafish without obvious harm before or after treating with ClO^-.

A novel "turn on" type fluorescent probe SE based on the thiophene carbazole derivative has been designed for sensing ClO^- *via* the appropriate ICT effect. SE exhibits outstanding ClO^- sensitivity and selectivity using both the green emission and the human eye without a UV light. By using ^1H NMR, HR-MS, and DFT calculations, it was confirmed that SE had an ICT response mechanism to ClO^-. In addition, SE has been used to identify endogenous ClO^- in zebrafish and living cells, and it is seen to be a promising approach for qualitatively monitoring the level of ClO^- in vivo.

Results and discussion

Synthesis of D-π-A compound

The precursor compound, 5-(6-octyl-6H-indolo[2,3-b]quinoxalin-9-yl)thiophene-2-carbaldehyde (**4**) was synthesized *via* modified literature procedure.[27,43] The synthesis begins

with the condensation reaction of 1,2-phenylene diamine and 5-bromo isatin in the presence of glacial aceticacid to get compound **1**. Compound **1** is then alkylated using n-octyl bromide in the presence of potassium carbonate in dimethylformamide (DMF) to get desired compound **2**. Compound 2 is stannylated using 2-tri(n-butyl)stannylthiophene in the presence of a palladium catalyst, $Pd(PPh_3)_4$. to get compound **3** Compound **3** is then subjected to formylation in the presence of phosphorus oxychloride in DMF. This formylation step introduces a formyl group (-CHO) into the molecule, leading to the formation of the desired product, compound **4**.

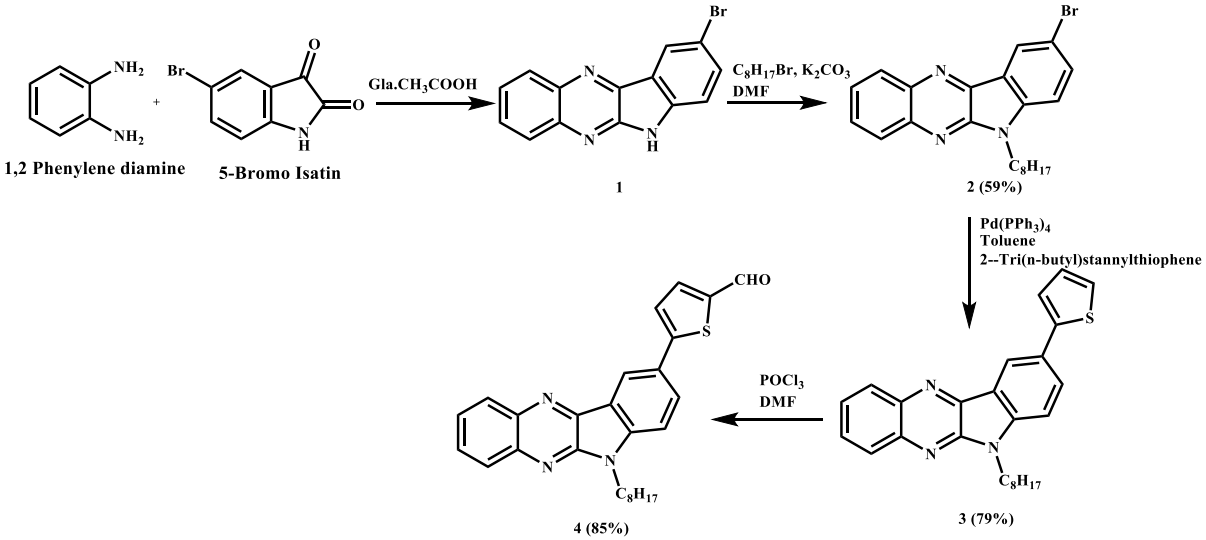

Scheme 5.1 Synthesis of 5-(6-octyl-6*H*-indolo[2,3-*b*]quinoxalin-9-yl)thiophene-2-carbaldehyde (**4**)

Compound **5** was synthesized according to the modified literature procedure reported by Li *et al*. [44,45] while compound **6** was synthesized according to the modified literature procedure reported by Bura *et al*.[46] 5-Bromoisatin is subjected to n-alkylation using potassium carbonate (K_2CO_3) and n-tetradecylbromide. The resulting compound **5** is subjected to Wolff-Kishner type reaction using hydrazine hydrate to get compound **6**.

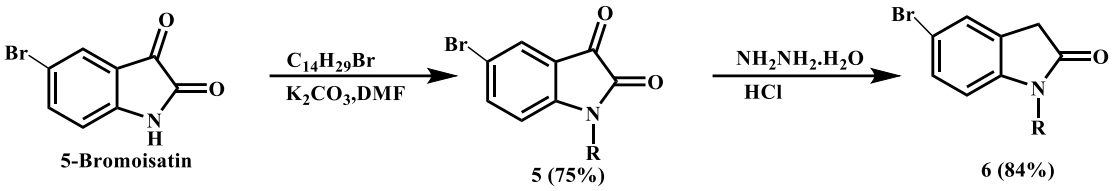

Scheme 5.2 Synthesis of 5-bromo-1-tetradecylindolin-2-one (**6**)

The compound **7** was synthesized by modified literature procedure reported by Milan *et al*.[47] by using N,N-dibutyl thiourea and diethyl malonate.

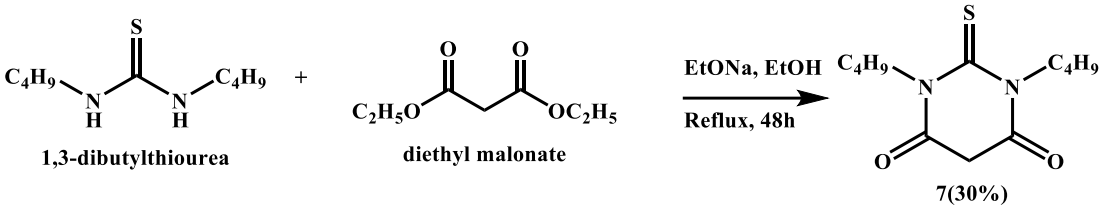

Scheme 5.3 Synthesis of 1,3-dibutyl-2-thioxodihydropyrimidine-4,6(*1H,5H*)-dione (**7**)

Compound **4** is being treated with various acceptor moieties (barbituric acid, thiobarbituric acid, and reduced isatin) under Knoevenagel condensation reaction conditions in the presence of piperidine to produce three different compounds, **IIQXN-BA**, **IIQXN-TBA**, and **IIQXN-RI**.

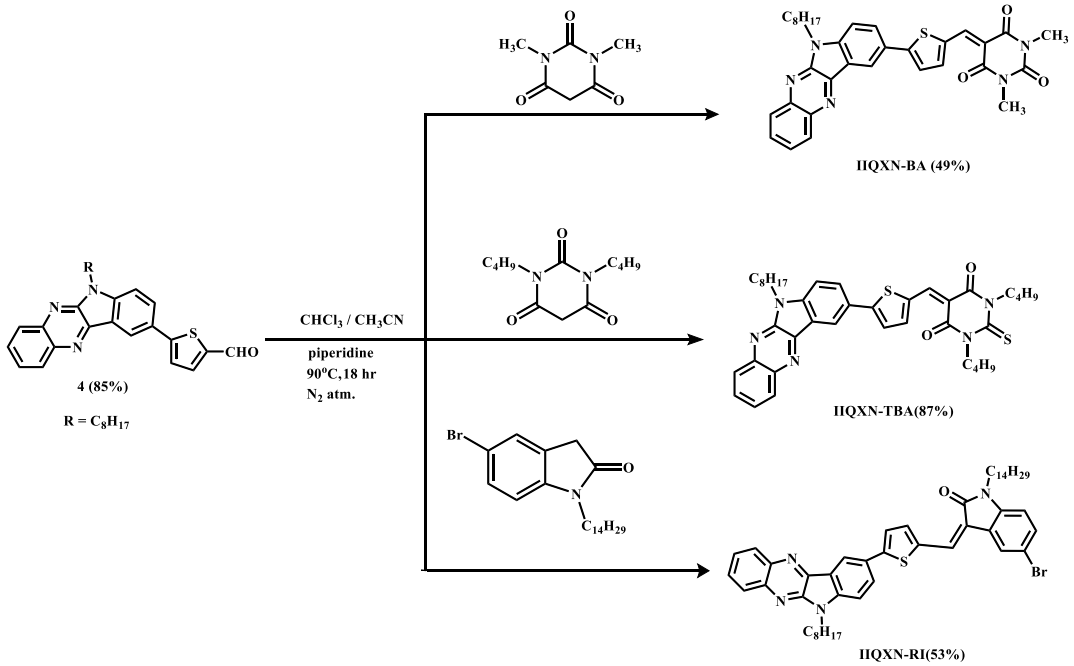

Scheme 5.4 Synthesis of compounds, **IIQXN-BA**, **IIQXN-TBA**, and **IIQXN-RI.**

Thermal properties of IIQXN-BA, IIQXN-TBA, and IIQXN-RI

Thermogravimetric analysis (TGA) was used to examine the thermal characteristics of all three compounds at a heating rate of 10 ℃/min in a nitrogen atmosphere. The temperature where a molecule loses 5% of its weight is known as the decomposition temperature (T_d). According to the TGA results, all three compounds, **IIQXN-BA**, **IIQXN-TBA**, and **IIQXN-RI** are thermally stable up to 345 ℃, 351 ℃, and 362 ℃, respectively (Figure 5.6), showing that they have high thermal stabilities.

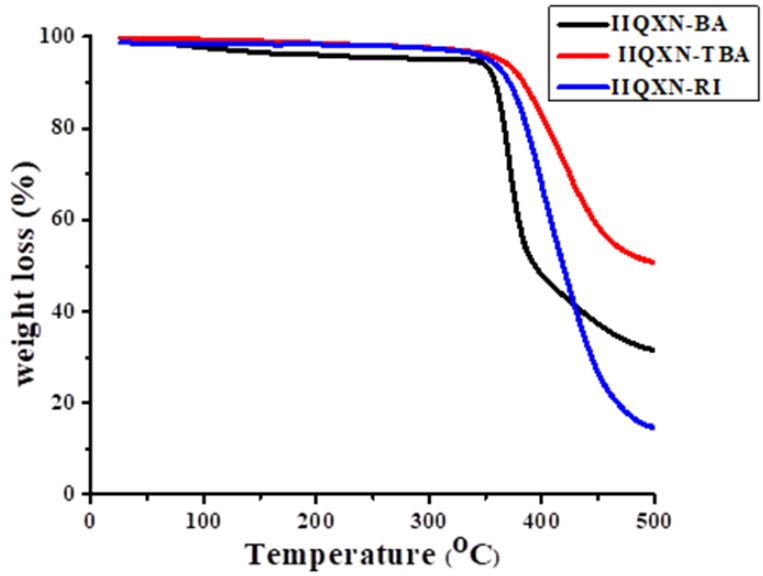

Figure 5.6 Thermogravimetric analysis (TGA) data of compound **IIQXN-BA** (black line), **IIQXN-TBA** (red line) and **IIQXN-RI** (blue line)

Photophysical properties of IIQXN-BA, IIQXN-TBA, and IIQXN-RI

The UV-Vis spectra were recorded on model Agilent Cary 60 UV-Visible spectrometer. Fluorescence spectra were recorded on a model HITACHI F-6300 fluorescence spectrometer. The quantum yield of the compounds was determined in chloroform solution using absorbance spectra, excitation wavelengths of emission spectra and integrated areas of the fluorescence-corrected spectra. Quinine sulphate was used as a reference ($\Phi s = 0.546$). The quantum yields were then calculated by using the following equation: $\phi x = \phi s \times (Ix/Is) \times (As/Ax) \times (nx/ns)^2$, Where x and s indicate unknown and standard solutions, respectively, ϕ is the quantum yield, I is the integrated area under the fluorescence spectra, A is the absorbance and n is the refractive index of the solvent. Compounds, **IIQXN-BA**, **IIQXN-TBA**, and **IIQXN-RI** were dissolve in $CHCl_3$ to prepare the corresponding stock solution (10 mM). Solvatochromism study

was carried out by varying the polarities of solvents. The different concentrations of hypochlorite (0-30 μM) were added into the solution of compounds, **IIQXN-BA**, **IIQXN-TBA**, and **IIQXN-RI** in quartz cuvette and subsequently UV-vis and fluorescence spectra were recorded in THF/water system.

UV-vis spectroscopy was used to conduct a photophysical analysis of all three compounds in diluted chloroform solution. Figure 5.7 depicts UV-vis absorption spectra of the molecules **IIQXN-BA**, **IIQXN-TBA**, and **IIQXN-RI**. Intermolecular charge transfer (ICT) causes the compounds **IIQXN-BA**, **IIQXN-TBA**, and **IIQXN-RI** to have wider peaks, with absorbance maxima at 476 nm, 508 nm, and 501 nm, respectively.

It was observed that when changing the acceptor from the barbituric acid moiety in compound **IIQXN-BA** to thiobarbituric acid moiety in compound **IIQXN-TBA** the ICT absorption band red-shifted by 32 nm from 476 nm to 508 nm, similar to that when changing the acceptor from the barbituric acid moiety in compound **IIQXN-BA** to reduced isatin moiety in compound **IIQXN-RI** the ICT absorption band red-shifted by 25 nm from 476 nm to 501 nm. The replacement of the acceptor group in **IIQXN-BA** with the thiobarbituric acid moiety in **IIQXN-TBA** results in a greater red-shift, indicating a more pronounced change in the electron distribution within the molecule. Similarly, when the acceptor group in **IIQXN-BA** is replaced with the reduced isatin moiety in **IIQXN-RI**, there is a red-shift, but it is not as significant as in the **IIQXN-TBA** case. This suggests that the reduced isatin moiety is somewhat less effective as an electron acceptor compared to the thiobarbituric acid moiety. This results indicates that the thiobarbituric acid group is the stronger electron withdrawing unit compare to barbituric acid and reduced isatin moiety.

In summary, the observed red-shifts in the ICT absorption bands when changing the acceptor groups indicate changes in the electron distribution within the compounds. The extent of the red-shift is influenced by the electron-accepting ability of the different acceptor groups (thiobarbituric acid moiety and reduced isatin moiety) relative to the barbituric acid moiety in compound **IIQXN-BA**.

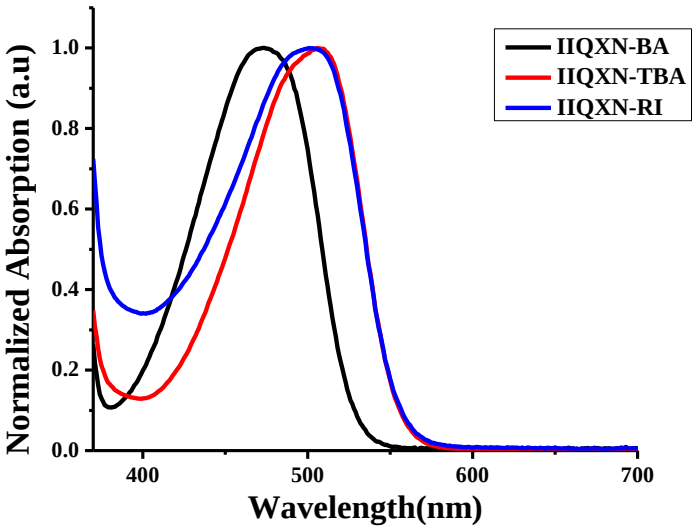

Figure 5.7 UV-Vis spectra of compounds, **IIQXN-BA**, **IIQXN-TBA**, and **IIQXN-RI**

In the emission spectra, upon low energy excitation of compound **IIQXN-BA** (λexc = 476), compound **IIQXN-TBA** (λexc = 508) and compound **IIQXN-RI** (λexc = 501), ICT emission was observed at 566 nm, 576 nm and 570 nm, respectively. When comparing the emission spectra, it can be seen that the ICT emission band red shifted from 566 to 574 nm by 8 nm when the acceptor was switched from barbituric acid in compound **IIQXN-BA** to thiobarbituric acid in compound **IIQXN-TBA**. On the other hand, after switching the acceptor from the reduced isatin in compound **IIQXN-RI** to the barbituric acid in compound **IIQXN-BA**, no noticeable alterations were noticed. These findings imply that the thiobarbituric acid moiety significantly red shifts ICT radiation. Compounds, **IIQXN-BA**, **IIQXN-TBA**, and **IIQXN-RI** were found to have quantum yields of 0.08, 0.13, and 0.04, respectively.

The sensing mechanism study of compound **IIQXN-BA** for ClO^-, ^1H NMR of compound **IIQXN-BA** after treatment with ClO^- was carried out. The solution of compound **IIQXN-BA** was mixed with ClO^- ion solution, and the resulting product was extracted using dichloromethane and used for ^1H NMR analysis. Following treatment with 30 μM of ClO^- ion solution, a new signal for the aldehyde group was found at 9.9 ppm, as seen in Figure 5.8. This finding suggested that ClO^- oxidised compound **IIQXN-BA**, cleaving the alkene double bond between the thiophene and pyrimidine moieties to form compound **IIQXN-ClO**. This alters the conjugated molecular electron arrangement and reduces the electron-donating capacity of the indoloquinoxaline moiety.

The fluorescence intensity of compound **IIQXN-BA** increased due to its D-π-A structure and a suitable ICT effect. A D-π-A structure typically refers to a molecule with a donor (D), a π-conjugated bridge (π), and an acceptor (A). This arrangement can lead to changes in electron density and energy levels within the molecule, resulting in changes in fluorescence properties. Similar behaviour to compound **IIQXN-BA** was observed for compound **IIQXN-RI**, particularly in its response to ClO^- (hypochlorite) in ^1H NMR spectra. This suggests that compound **IIQXN-RI** may also have a "D-π-A" structure and an ICT effect that influences its fluorescence properties.

In contrast to **IIQXN-BA** and **IIQXN-RI** compound **IIQXN-TBA** showed a decrease in fluorescence intensity. This decrease is attributed to the "cleavage of alkene unit" between the thiophene and pyrimidine moieties. The cleavage of the alkene bond can disrupt the conjugation of electrons in the molecule, leading to changes in its fluorescence behaviour. This change may be due to the alteration of the electronic structure of molecules, which affects its ability to emit fluorescence. How different structural and chemical changes in these compounds are impacting their fluorescence properties, with compound **IIQXN-BA** and **IIQXN-RI** showing increased fluorescence intensity due to their "D-π-A" structures and ICT effects, while compound **IIQXN-TBA** is experiencing decreased fluorescence due to the cleavage of an alkene bond in its structure.

Furthermore, the LCMS investigation provided additional evidence about the ClO^-sensing mechanism. The mass spectra of compound **IIQXN-BA** were examined both with and without ClO^- treatment. Molecular ion peak of **IIQXN-BA** was discovered at m/z 580.2357 ($[M1 + H]^+$), as Figure 5.9(a) illustrates. Following the ClO^- treatment, the LCMS of **IIQXN-BA** was determined to be at m/z 442.6264 Figure 5.9(b), corresponding to the iconic peak of the anticipated product **IIQXN-ClO** (estimated for 442.1908 [**IIQXN-ClO** + H]$^+$). This result further proves the sensing mechanism is that ClO^-.

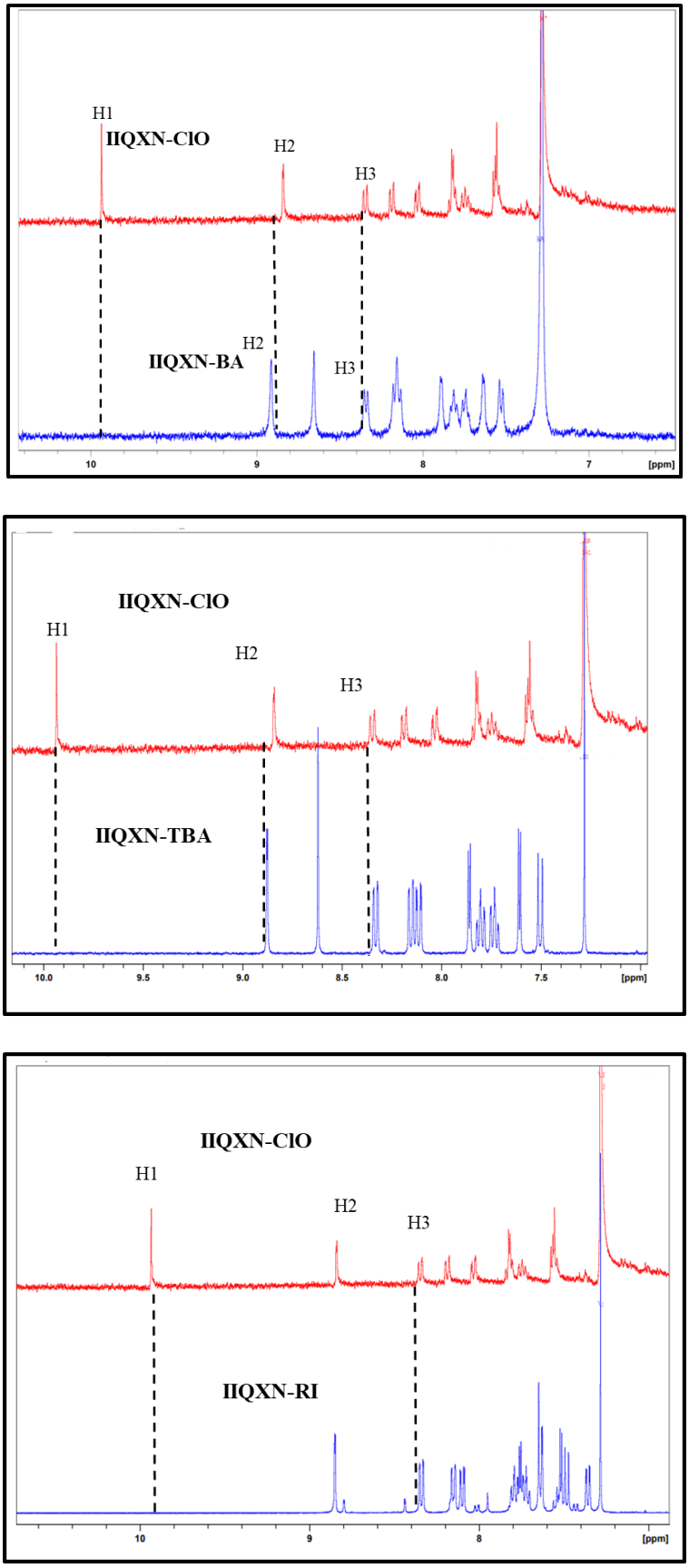

Figure 5.8 ^{1}H NMR spectra of compound **IIQXN-BA**, **IIQXN-TBA**, and **IIQXN-RI (Blue line)** and compound **IIQXN -ClO (Red line)** (after treatment of 30 µM of ClO^{-}).

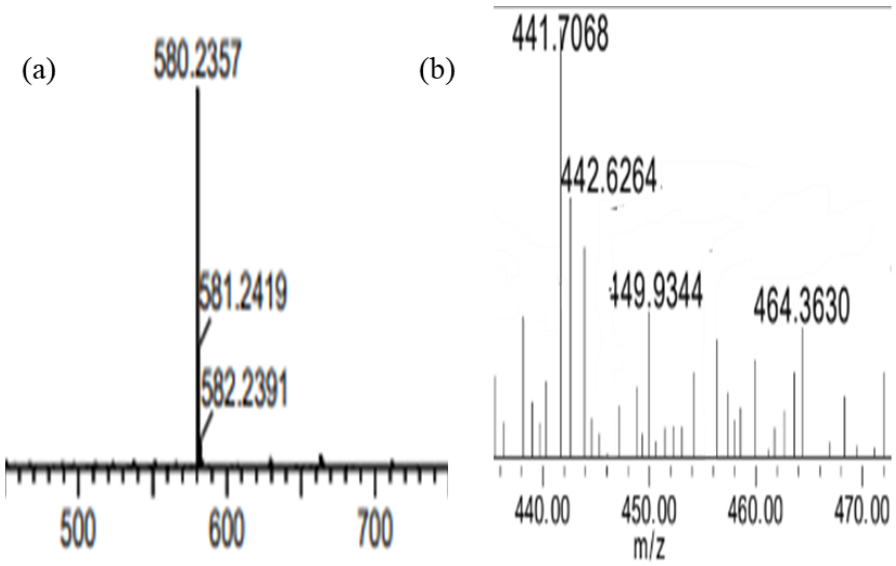

Figure 5.9 (a) Mass spectra of compound **IIQXN-BA** and (b) Mass spectra of compound **IIQXN-ClO** (after treating compound **IIQXN-BA** with ClO^-).

Electrochemical properties

The electrochemical studies are conducted using an Electro Chemical Analyzer, Model SP-200, made by Biologics Sas France. Platinum (Pt) disk is used as the working electrode. Pt electrodes are commonly used in electrochemical studies due to their inert nature. Platinum wire serves as the counter electrode. The counter electrode facilitates the flow of current in the electrochemical cell. AgCl-coated Ag wire is used as the reference electrode. Ag/Ag+ electrodes are often employed as reference electrodes in non-aqueous electrochemical studies. A non-aqueous Ag/Ag+ wire is prepared by dipping a silver wire into a solution of $FeCl_3$ and HCl. The Pt-disk electrodes are polished with alumina to ensure a clean and smooth surface. They are then washed with water and acetone to remove any contaminants. Finally, they are dried with nitrogen gas to eliminate any residual moisture or oxygen. All electrochemical potentials are reported against Ag/Ag+ as the reference electrode, and ferrocene (Fc/Fc+) is used as an external standard. The onset potential for ferrocene is noted as $E_{(onset(Fc/Fc+)} = 0.50$ V). This standard provides a reference point for measuring potentials.

Cyclic voltammetric (CV) experiments are conducted in a solution composed of dry chloroform and acetonitrile in a 7:3 ratio. Tetra-n-butylammonium hexafluorophosphate ($TBAPF_6$) is used as the supporting electrolyte. Supporting

electrolytes enhance the ionic conductivity of the solution, facilitating electrochemical reactions.

All the synthesised compounds showed irreversible oxidation and reduction potential as shown in Figure 5.10. The oxidation potential of compounds, **IIQXN-BA**, **IIQXN-TBA**, and **IIQXN-RI** are measured from oxidation waves and are found to be at +0.49, +0.48 and +0.45 respectively with the onset oxidation potential values of +0.43, +0.39 and +0.38 respectively. The HOMO energy levels are calculated from onset oxidation values and the values are found to be at −4.73, −4.69 and −4.68, respectively. The reduction potential of compounds, **IIQXN-BA**, **IIQXN-TBA**, and **IIQXN-RI** are measured from reduction waves and the values are found to be at −0.47, −0.50 and −0.48 with the onset reduction potential values of −0.87, −0.88 and −0.88, respectively. The LUMO energy levels are calculated from onset reduction potential values and they are found to be at −3.43, −3.42 and −3.42, respectively. The electrochemical properties of all the molecules are summarized in Table 5.1.

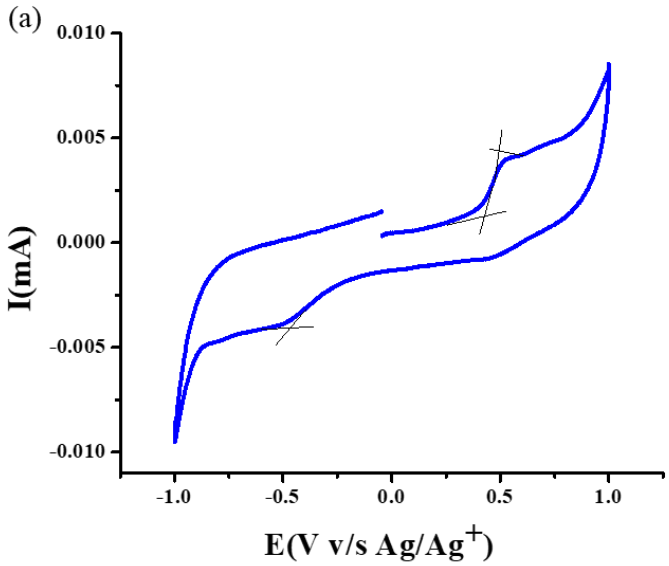

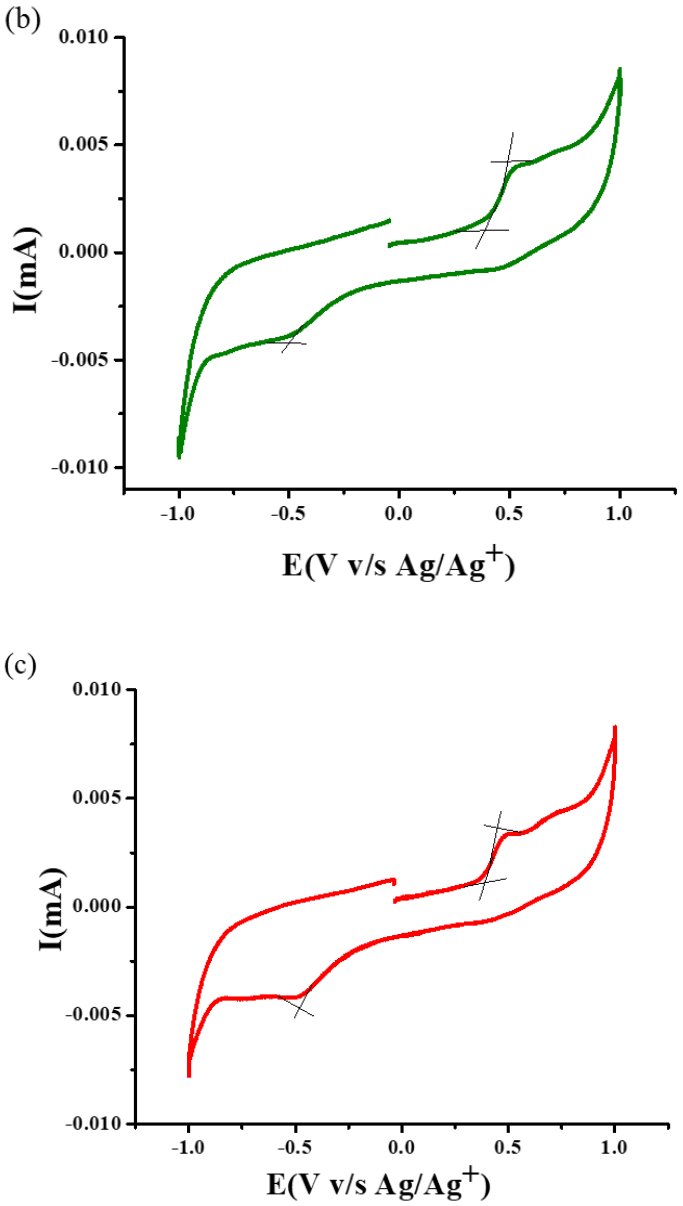

Figure 5.10 Oxidation curves of and reduction curves of (a) compound **IIQXN-BA**, (b) compound **IIQXN-TBA** and (c) compound **IIQXN-RI** obtained by cyclic voltammetry at 50 mV/s in dry acetonitrile-chloroform (7:3) system using $TBAPF_6$ as supporting electrolyte; $\boldsymbol{E_{onset\,Fc/Fc^+} = 0.50\,V}$.

Table 5.1 Electrochemical properties of compounds, **IIQXN-BA**, **IIQXN-TBA**, and **IIQXN-RI**

Compound	E_{oxi} (V) [a]	$E_{onset\ oxi}$ (V) [a]	E_{HOMO} (eV) [b]	E_{red} (V) [a]	$E_{onset\ red}$ (V) [a]	E_{LUMO} (eV) [b]
IIQXN-BA	+0.49	+0.43	−4.73	-0.47	−0.87	−3.43
IIQXN-TBA	+0.48	+0.39	−4.69	-0.50	−0.88	−3.42
IIQXN-RI	+0.45	+0.38	−4.68	-0.48	−0.88	−3.42

[a]potential v/s Ag/Ag^+; [b]calculated from equation $E_{HOMO} = -(E_{onset\ oxi} + 4.8 - E_{onset\ Fc/Fc^+})$; [c] calculated from equation $E_{LUMO} = -(E_{onset\ red} + 4.8 - E_{onset\ Fc/Fc^+})$.

Computational studies

Density functional theory (DFT) is a computational quantum mechanical method used to study the electronic structure of molecules and materials. This level of theory provides a reasonable balance between accuracy and computational cost. Theoretical calculations for three compounds, **IIQXN-BA**, **IIQXN-TBA**, and **IIQXN-RI** were carried out by using the B3LYP/6-31G(d) basic set using Gaussian 16.

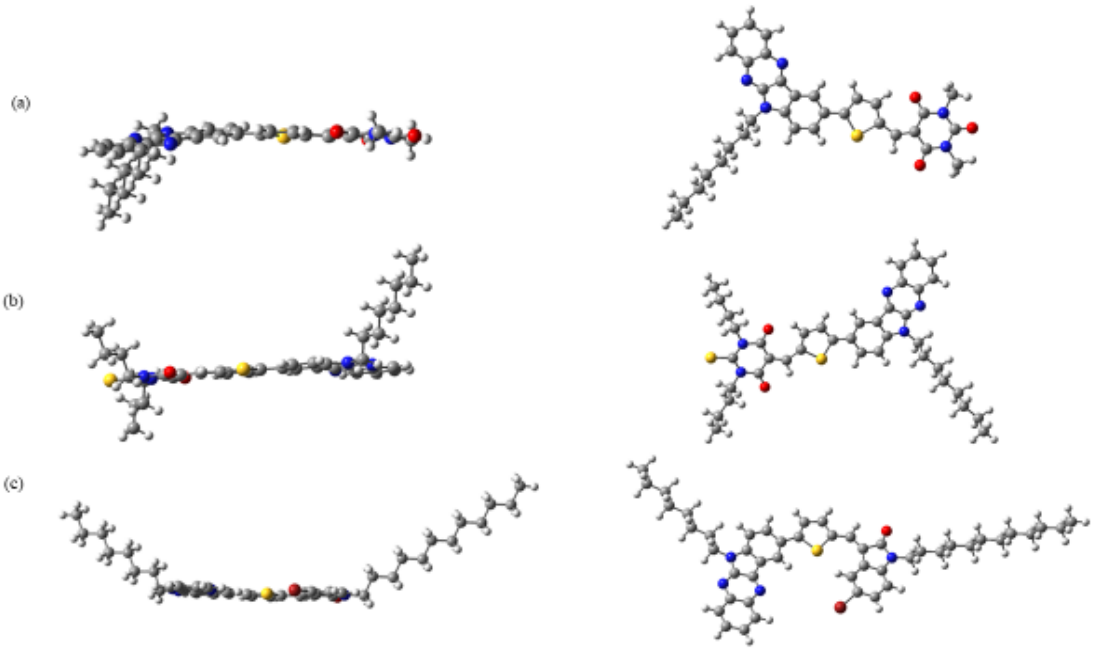

Figure 5.11 DFT optimised structure of (a) compound **IIQXN-BA**, (b) compound **IIQXN-TBA** and (c) compound **IIQXN-RI** by using Gaussian B3LYP/6-31G point group

For compounds **IIQXN-BA**, **IIQXN-TBA**, and **IIQXN-RI**, the HOMO are spread across the entire molecules. the LUMO of these compounds mainly focus on the indoloquinoxaline unit. But for **IIQXN-ClO**, both the HOMO and LUMO are distributed throughout the entire conjugated system of the molecule.

The band gap value is the energy difference between the HOMO and LUMO, and it provides insights into the compound's electronic properties. The band gap value for compound **IIQXN-ClO** is 3.40 eV. The band gap values for compounds, **IIQXN-BA**, **IIQXN-TBA**, and **IIQXN-RI** are 2.87 eV, 2.69 eV, and 2.88 eV, respectively. The data indicates that **IIQXN-ClO** has a larger band gap (3.40 eV) compared to **IIQXN-BA**, **IIQXN-TBA**, and **IIQXN-RI**, which have band gap values in the range of 2.69 to 2.88 eV. A larger band gap generally suggests that **IIQXN-ClO** is less conductive and has a higher energy barrier for electronic transitions compared to **IIQXN-BA**, **IIQXN-TBA**, and **IIQXN-RI**. The electronic properties and band gap values of these compounds can provide insights into their potential applications, especially in areas, such as semiconductors, optoelectronics, or materials science, depending on the specific properties and intended use of these molecules.

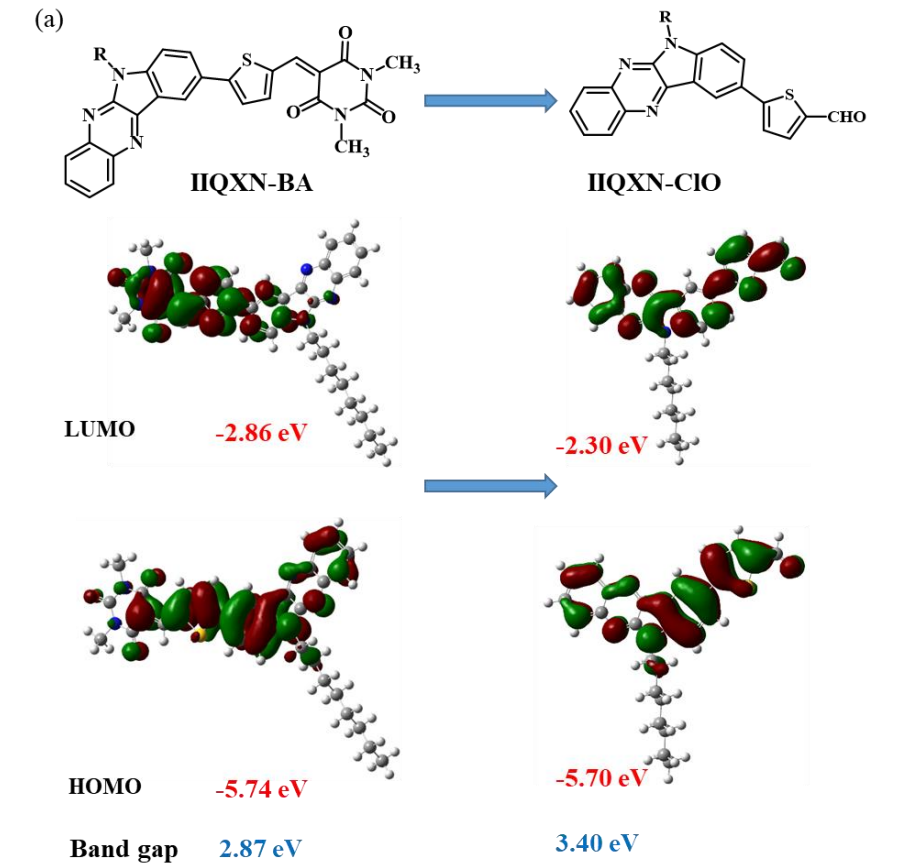
(a)
IIQXN-BA
IIQXN-ClO
LUMO
-2.86 eV
-2.30 eV
HOMO
-5.74 eV
-5.70 eV
Band gap
2.87 eV
3.40 eV

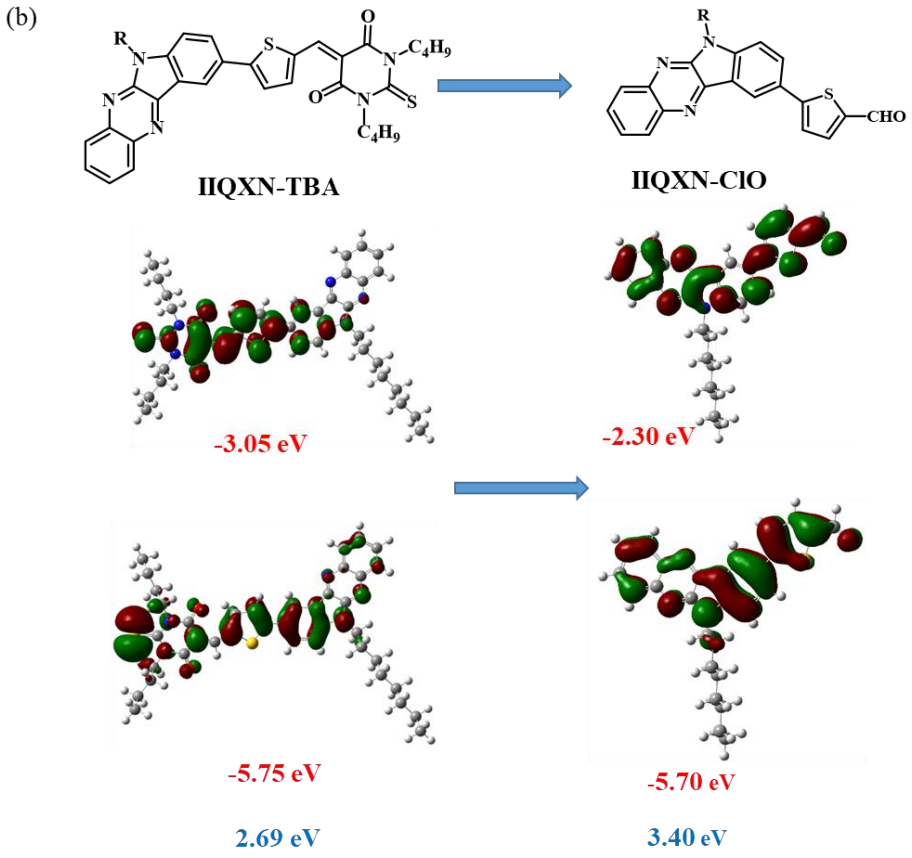
(b)
IIQXN-TBA
IIQXN-ClO
-3.05 eV
-2.30 eV
-5.75 eV
-5.70 eV
2.69 eV
3.40 eV

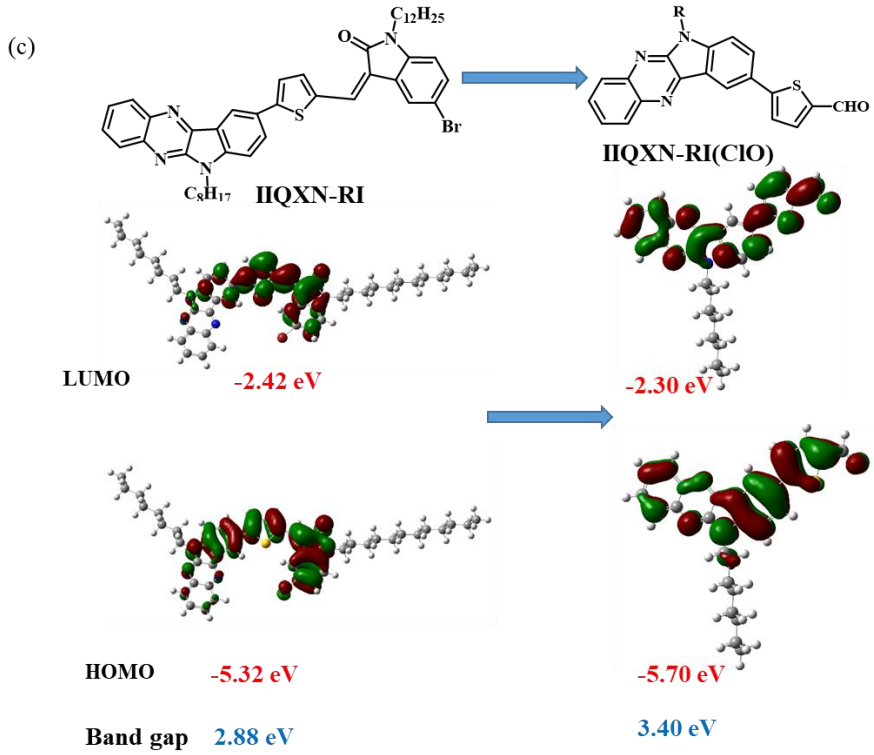

Figure 5.12 HOMO-LUMO energy level diagram of compounds **IIQXN-BA**, **IIQXN-TBA**, and **IIQXN-RI** and **IIQXN-ClO** using Gaussian B3LYP/6-31G.

Conclusion

Three novel indoloquinoxaline-based D-π-A molecules **IIQXN-BA**, **IIQXN-TBA**, and **IIQXN-RI** were synthesized and characterized using various spectroscopic techniques. These compounds were investigated for their ability to detect ClO^- ions, and the findings indicate their sensitivity and selectivity in this regard. Characterization of all the three compounda **IIQXN-BA**, **IIQXN-TBA**, and **IIQXN-RI** was performed using techniques such as IR NMR, and HRMS. All three synthesized compounds (**IIQXN-BA**, **IIQXN-TBA**, and **IIQXN-RI**) exhibited excellent sensitivity and selectivity towards ClO^- ions. The detection was achieved through green emission, which was visible to the naked eye. Compound **IIQXN-BA** and compound **IIQXN-RI** showed a "TURN ON" type of fluorescent probe behavior in response to ClO^- ions. Compound **IIQXN-TBA** exhibited a "TURN OFF" type of fluorescent probe behavior upon interaction with ClO^- ions. The mechanism of intramolecular charge transfer (ICT) towards ClO^- ions was confirmed through ^1H NMR and mass analysis studies. The molecules were subjected to electrochemical studies, revealing HOMO energy

levels at approximately -5.1 eV and LUMO energy levels at approximately -3.4 eV. The theoretical band gap value for the **IIQXN-ClO** was found to be 3.40 eV, while the band gap values for compounds **IIQXN-BA**, **IIQXN-TBA**, and **IIQXN-RI** were 2.87 eV, 2.69 eV, and 2.88 eV, respectively. All three compounds exhibited good thermal stability above 300°C.

Overall, in this study, a detailed characterization of the synthesized molecules and their promising properties as fluorescent probes for the detection of ClO^- ions was carried out .

Experimental procedures

General procedure

All the reagent-grade chemicals were used as purchased. The reactions were performed under an inert atmosphere of dry nitrogen to prevent the presence of moisture, which can interfere with certain reactions. Solvents used in the reactions were dried to remove any traces of moisture or impurities. Merck silica gel 60 F-254 thin-layer plates were used for monitoring reactions. Infrared spectra were recorded using a Perkin-Elmer FTIR RXI spectrometer with KBr pellets. NMR (^{1}H & ^{13}C) spectra were recorded on a Bruker AV-III spectrometer using $CDCl_3$ as the solvent. HRMS data were recorded on an Xevo G2-XS QTOF Mass Spectrometer Absorption spectra in the UV-Visible range were recorded using an Agilent Cary 60 Spectrophotometer. Fluorescence data were recorded on a Jasco FP 6300 Spectrofluorometer using a quartz cuvette. Electrochemical analyses were carried out using an Electro Chemical Analyser, Model SP-200, with specific electrode setups.

Synthesis of 5-(6-octyl-6*H*-indolo[2,3-*b*] quinoxalin-9-yl)thiophene-2-carbaldehyde

Compound **2** was synthesized according to the modified literature procedure reported by Abby *et al.*[43] and formylation was carried out according to modified literature procedure reported by Venkateswara Rao *et al.*[49]

Synthesis of 9-bromo-6*H*-indolo[2,3-*b*]quinoxaline (1): Benzene-1,2-diamine (0.49 g, 4.60 mmol), 5-bromoisatin (1.00 g, 4.40 mmol) and acetic acid (167 mL) was taken in 250 mL two necked round bottom flask. Reaction mixture was refluxed at 150 ℃ under nitrogen atmosphere and stirred for 20h. After cooling to room temperature, the reaction mixture was poured into crushed ice and filtered with a Buckner funnel, dried the compound to get a greenish yellow precipitates of 9-bromo-6*H*-indolo[2,3-*b*]quinoxaline (**1**) with a yield of 97% (1.27 g). The solid product was directly used for the next step without further purification.

Synthesis of 9-bromo-6-octyl-6*H*-indolo[2,3-*b*]quinoxaline (2): Compound **1** (1.15 g, 4.26 mmol), K_2CO_3 (1.61 g, 1.20 mmol) and 8 mL of DMF were taken in 100 mL two neck round bottom flask. 1-Bromooctane (1 mL, 5.70 mmol) was added to the reaction mixture under nitrogen atmosphere. The mixture was allowed to stir at 140 ℃ for 12h under a nitrogen atmosphere. After cooling to room temperature, the solution

was poured into brine solution, stirred for 15 minutes, and then extracted with ethyl acetate. The combined organic layer was dried over anhydrous Na_2SO_4, filtered and evaporated to dryness. The crude product was purified by column chromatography over silica gel using petroleum ether/ethyl acetate (20:1) solvent mixture as an eluent. 9-bromo-6-octyl-6*H*-indolo[2,3-*b*]quinoxaline (**2**) was obtained as yellow solid after drying under vacuum.

9-Bromo-6-octyl-6*H*-indolo[2,3-*b*]quinoxaline (2): Yellow solid (59%, 0.95 g); ^{1}H NMR (400 MHz, $CDCl_3$) δ: 8.61 (s, 1H), 8.28-8.30 (d, 1H), 8.13-8.15 (d, 1H), 7.76-7.80 (t, 2H), 7.68-7.72 (t, 1H), 7.36-7.38 (d, 1H), 4.05-4.08 (t, 2H) 2.06 (s, 2H), 1.35-1.38 (d, 4H), 1.25-1.29 (m, 6H), 0.86-0.89 (t, 3H).

Synthesis of 9-thiophene-6-octyl-6*H*-indolo[2,3-*b*]quinoxaline (3): 9-Bromo-6-octyl-6*H*-indolo[2,3-*b*]quinoxaline (**2**) (0.50 g, 1.2 mmol) was dissolved in toluene (10 mL) and stirred at room temperature for 10 minutes under nitrogen atmosphere. $Pd(PPh_3)_4$ (10 mol%, 139 mg) was added to the reaction mixture which was then purged with nitrogen atmosphere for 10 minutes. Tributyl(thiophen-2-yl)stannane (0.45 mL, 1.4 mmol) was slowly added and the resulting mixture was then stirred at 90 ℃ for 14h under nitrogen atmosphere. The reaction mixture was poured into crushed ice and extracted with ethyl acetate. The combined organic layers were washed with 2% aqueous $NaHCO_3$ solution followed by brine and dried over anhydrous Na_2SO_4. The solvent was removed under reduced pressure and the crude product was purified by column chromatography over silica gel using petroleum ether/ethyl acetate (50:1) solvent mixture as an eluent. 9-Thiophene-6-octyl-6*H*-indolo[2,3-*b*]quinoxaline (**3**) was obtained as dark yellow solid after drying under vacuum.

9-Thiophene-6-octyl-6*H*-indolo[2,3-*b*]quinoxaline (3): Dark yellow solid (79%, 0.40 g); ^{1}H NMR (400 MHz, CDCl3) δ 8.73 (s, 1H), 8.31-8.34 (d, 1H), 8.14-8.17 (d, 1H), 7.94-7.96 (d, 1H), 7.76-7.80 (m, 1H), 7.68-7.72 (m, 1H), 7.46-7.49 (dd, J=3.6 Hz, 1H), 7.42-7.43 (d, 1H), 7.28-7.32 (dd, 1H), 7.14 (m, 1H), 4.47-4.513 (t, 2H), 1.93-1.97 (sext, 2H), 1.39-1.44 (m, 4H), 1.23-1.30 (m, 6H), 0.87-0.90 (t, 3H).

Synthesis of 5-(6-Octyl-6*H*-indolo[2,3-*b*]quinoxaline)-thiophene-2-carbaldehyde (4): DMF (0.17 mL, 4.38 mmol) was taken in 50 mL clean dry two neck round bottom flask and cooled in ice-salt bath under nitrogen atmosphere. To this $POCl_3$ (0.204 mL, 4.38 mmol) was added and the mixture was stirred at 0 ℃ for 2 h. To this mixture,

solution of 9-thiophene-6-octyl-6*H*-indolo[2,3-*b*]quinoxaline (**3**) (0.30 g, 0.73 mmol) in dichloromethane (DCE)) (22 mL) was added dropwise with the help of syringe through a rubber septum. Reaction mixture was stirred at room temperature for 1h and then refluxed at 84 ℃ for 24 h. After completion of reaction, water was added to the reaction mixture and stirred for 10 minutes. The desired product was separated by vacuum filtration and washed with methanol. Compound **4** was obtained as yellow solid with 85% (0.27 g) of yield.

5-(6-Octyl-6*H*-indolo[2,3-*b*]quinoxaline)-thiophene-2-carbaldehyde (4): Fluorescent yellow solid (85%, 0.27 g); ^{1}H NMR (400 MHz, $CDCl_3$) δ: 9.92 (s, 1H), 8.79 (s, 1H), 8.32-8.34 (d, 1H), 8.16-8.18 (d, 1H), 7.98-8.00 (d, 1H), 7.79-7.83 (t, 1H), 7.71-7.75 (t, 1H), 7.52-7.54 (t, 2H), 7.28 (s, 1H), 4.49-4.53 (t, 2H), 1.96-1.99 (t, 2H), 1.40 (s, 4H), 1.26(s, 6H), 0.85-0.86 (t, 3H).

Synthesis of 5-bromo-1-tetradecylindolin-2-one

Compound **5** was synthesized according to the modified literature procedure reported by Li *et al*. [44,45] while compound **6** was synthesized according to the modified literature procedure reported by Bura *et al*. [46]

Synthesis of 5-bromo-1-tetradecylindoline-2,3-dione (5): 5-Bromoisatin (2 g, 8.84 mmol) and potassium carbonate (K_2CO_3) (5.48g, 39.7 mmol) was added to 20 mL anhydrous DMF under nitrogen atmosphere and the reaction mixture was stir at 60 ℃ for 10-15 minutes. To this stirred solution, *n*-tetradecyl bromide (4.2 g ,15.47 mmol) was added in a dropwise manner. The resultant reaction mixture was allowed to stir at 80 ℃ for 3h, after cooling to room temperature, the resultant reaction mixture was poured in to water and extracted with ethyl acetate. The combined organic layer was washed with water and dried over Na_2SO_4 and solvent was evaporated under reduced pressure. The crude product was purified by column chromatography over silica gel and pure product was eluted using ethyl acetate/petroleum ether (1:10) as a mobile phase.

5-Bromo-1-tetradecylindoline-2,3-dione (5): Dark orange solid. (1.83 g, 49%); ^{1}H NMR (400 MHz, $CDCl_3$) δ: 7.67 (d, J3 = 1.2 Hz, 1H), 6.79 (d, J2 = 7.6 Hz, 1H), 6.82 (dd, 1H), 3.70−3.74 (t, 2H), 1.65−1.73 (m, 2H), 1.29−1.34 (m, 18H), 0.85−0.89 (t, 3H).

Synthesis of 5-bromo-1-tetradecylindolin-2-one (6): Compound 5 (1.5g, 3.55mmol) and hydrazine hydrate 99% (8.88g, 177.5mmol) was taken in a two necked round

bottom flask and refluxed at 140 ℃ for 1h. After cooling to room temperature the reaction mixture was poured in to water and extracted with ethyl acetate, washed with water and dried over anhydrous sodium sulphate, Solvent was evaporated under reduced pressure. To the resulting crude product, 20 mL of 6N aqueous hydrochloric acid is added and the resulting mixture was heated at 60 ℃ for 3h. The reaction mixture was poured in to 200 mL of water and extracted with ethyl acetate. Combined organic layer was washed with water followed by brine and dried over anhydrous sodium sulphate. The solvent was evaporated under reduced pressure. The crude product was purified by column chromatography over silica gel and pure product was eluted using ethyl acetate/petroleum ether (4:10) as a mobile phase

5-Bromo-1-tetradecylindolin-2-one (6): Pale yellow solid. (1.24 g, 84%); ^{1}H NMR (400 MHz, $CDCl_3$) δ: 7.39 (d, 1H), 7.26 (s, 1H), 6.768 (d, 1H), 3.65−3.68 (t, 2H), 3.51 (s, 2H), 1.62−1.66 (m, 2H), 1.25−1.32 (m, 18H), 0.86−0.90 (t, 3H).

Synthesis of 1,3-dibutyl-2-thioxodihydropyrimidine-4,6(1*H*,5*H*)-dione

The compound **7** was synthesised by modified literature procedure reported by Milan *et al*.[47] by using N,N-dibutyl thiourea and diethyl malonate. Take 20 mL ethanol in a two necked round bottom flask and cool it to 0 ℃. Add Na-metal (0.7g, 30.4mmol) in portion wise under nitrogen atmosphere and stir the reaction mixture until the Na-metal dissolves. After that N, N-dibutyl thiourea (1.0g, 5.45mmol) and diethyl malonate (1.74 g, 10.9 mmol) was added and stir the reaction mixture for 20 minutes. Reflux the reaction mixture for 48h. Cool the reaction mixture and evaporate the excess of ethanol. Add water (200 mL) to get precipitate of product and filter the product. The filtrate was acidified with (1:1) HCl and extract the product with dichloromethane (DCM). Combined organic layer was washed with water, followed by brine, dried over anhydrous sodium sulphate and evaporated under reduced pressure. The crude product was purified by column chromatography over silica gel and pure product was eluted using ethyl acetate-petroleum ether (3:10) as a mobile phase

1,3-Dibutyl-2-thioxodihydropyrimidine-4,6(1*H*,5*H*)-dione (7): White solid. (0.41 g, 30%) ^{1}H NMR (400 MHz, CDCl3) δ: 4.35-4.31 (s, 2H), 3.70 (s, 1H), 1.41 (t, 2H), 1.38 (t, 2H), 0.97 (s, 3H).

Synthesis of IIQXN-BA, IIQXN-TBA, and IIQXN-RI

Synthesis of 5-((6-octyl-6H-indolo[2,3-b]quinoxaline-9-yl)-thiophene-2-yl)-1,3-dimethylpyrimidine-2,4,6(1H,3H,5H)-trione (IIQXN-BA): A mixture of compound **4** (100 mg, 0.22 mmol), 1,3-dimethylbarbituric acid (42.3 mg, 0.27 mmol) are first taken in two necked round bottom flask containing acetonitrile (15 mL) and chloroform (15 mL) and stirred at room temperature under nitrogen atmosphere. After the solution has become completely transparent, heating was started and piperidine (0.054 mL, 0.54 mmol) was added immediately. The resulting reaction mixture was refluxed at 90 ℃for 18h under nitrogen atmosphere. After cooling to room temperature, the bright orange solid started to precipitate out. The resulting solid was filtered and washed thoroughly with water. Then, the crude product was purified by crystallization in ethanol.

5-((6-Octyl-6*H*-indolo[2,3-*b*]quinoxaline-9-yl)-thiophene-2-yl)-1,3-dimethylpyrimidine-2,4,6(1*H*,3*H*,5*H*)-trione (IIQXN-BA): Orange solid (64 mg, 49.2%), ^{1}H NMR (400 MHz, $CDCl_3$)÷ δ: 8.87 (s, 1H), 8.62 (s, 1H), 8.34-8.31 (d, J=12Hz, 1H), 8.16-8.10 (q, J=24Hz, 2H), 7.86-7.85 (d, J=4Hz, 1H), 7.82-7.80 (t, J=8Hz, 1H), 7.78-7.71 (t, 1H), 7.61-7.60 (d, J=4Hz, 1H), 7.51-7.49 (d, J=8Hz, 1H), 4.52-4.48 (s, 2H), 3.46-3.43 (s, 6H), 1.99-1.94 (m, 2H), 1.67 (m, 4H), 1.45-1.41 (m, 7H), 1.29-1.26 (m, 3H). ^{13}C NMR (100 MHz, $CDCl_3$): δ 162.9, 161.8, 1605, 151.8, 148.3, 147.1, 145.9, 144.7, 141.2, 139.2, 138.8, 135.7, 129.2, 128.0, 126.5, 125.7, 123.6, 120.9, 119.7, 109.8, 109.9, 42.0, 31.8, 29.3, 28.6, 28.2, 27.8, 23.9, 13.9. HRMS (ES+): $C_{33}H_{34}N_5N_5O_3S$ requires 580.2382, found 580.2357. IR (KBr, cm^{-1}): 3424.88, 3006.18, 2924.18, 2852.44, 1727.07, 1700.55, 1612.08, 1582.10, 1511.80, 1474.49, 1428.16, 1404.13, 1350.75, 1313.98, 1253.26, 1205.87, 1123.46, 1043.59, 976.40, 950.16, 815.42, 769.16, 722.29, 639.1, 587.83, 526.15, 455.83.

Synthesis of 1,3-Dibutyl-5-((5-(6-octyl-6H-indolo[2,3-b]quinoxalin-9-yl)thiophen-2-yl) methylene)-2-thioxodihydropyrimidine-4,6(1H,5H)-dione (IIQXN-TBA): A mixture of compound **4** (100 mg, 0.22 mmol), 1,3-dibutylthiobarbituric acid (35.01 mg, 0.27 mmol) are first taken in two necked round bottom flask containing acetonitrile (15 mL) and chloroform (15 mL) and stirred at room temperature under nitrogen atmosphere. After the solution has become completely transparent, heating was started and piperidine (0.054 mL, 0.54 mmol) was

added immediately. The resultant reaction mixture was refluxed at 90 ℃ for 18h under nitrogen atmosphere. After cooling to room temperature, the bright orange solid started to precipitate out. The resulting solid was filtered and washed thoroughly with water. The crude product was further purified by crystallization in ethanol.

1,3-Dibutyl-5-((5-(6-octyl-6*H*-indolo[2,3-*b*]quinoxalin-9-yl)thiophen-2-yl)methylene)-2-thioxodihydropyrimidine-4,6(1*H*,5*H*)-dione (IIQXN-TBA): Dark orange solid (87.62 mg, 57%), ^{1}H NMR (400 MHz, $CDCl_3$) δ: 8.91 (s, 1H), 8.65 (s, 1H), 8.35-8.33 (d, J=8Hz, 1H), 8.17-8.13 (t, J=16Hz, 2H), 7.89 (d, 1H), 7.81-7.74 (2H), 7.64 (d, 1H), 7.55-7.52 (d, J=12Hz, 1H), 4.52 (s, 2H), 3.48-3.44 (s, 6H), 1.98 (2H), 1.67 (m, 10H), 1.42 (m, 4H), 1.26 (m, 11H), 0.87 (s, 5H). ^{13}C NMR (100 MHz, $CDCl_3$) δ: 182.8, 162.1, 155.4, 154.6, 145.9, 145.5, 142.3, 142.0, 140.7, 139.6, 139.1, 138.3, 128.5, 127.7, 126.5, 123.7, 120.5, 120.1, 119.3, 45.6, 41.7, 32.1, 29.8, 29.0, 26.2, 23.0, 21.8, 20.6, 19.8, 18.2, 14.3, 13.1. HRMS(ES+): $C_{39}H_{45}N_5O_2S_2$ requires 680.3015, found 680.4463. IR (KBr, cm^{-1}): 3430.17, 2952.27, 2853.90, 2808.27, 2737.49, 2625.26, 2511.74, 2412.54, 2315.35, 1725.09, 1622.22, 1587.21, 1453.63, 1399.33, 1284.75, 1207.28, 1120.86, 1030.18, 850.37, 950.37, 771.02, 549.03**.**

Synthesis of 5-bromo-1-dodecyl-3-((5-(6-octyl-6H-indolo[2,3-b]quinoxalin-9-yl)thiophen-2-yl)methylene)indolin-2-one (IIQXN-RI): A mixture of compound **4** (100 mg, 0.23 mmol), reduced isatin (143 mg, 0.27 mmol) are first taken in two necked round bottom flask containing acetonitrile (15 mL) and chloroform (15 mL) and stirred at room temperature under nitrogen atmosphere. After the solution has become completely transparent, heating was started and piperidine (0.054 mL, 0.54 mmol) was added immediately. The resultant reaction mixture was refluxed at 90 ℃ for 18h under nitrogen atmosphere. After cooling to room temperature, the bright orange solid started to precipitate out. The resulting solid was filtered and washed thoroughly with water. The crude product was further purified by crystallization in ethanol.

5-Bromo-1-dodecyl-3-((5-(6-octyl-6*H*-indolo[2,3-*b*]quinoxalin-9-yl)thiophen-2-yl)methylene)indolin-2-one (IIQXN-RI): Dark red solid (99 mg, 53%), ^{1}H NMR (400 MHz, $CDCl_3$): δ 8.85-8.84 (s, J=4Hz, 1H), 8.35-8.33 (d, J=8Hz, 1H), 8.16-8.07(dd, 2H), 7.79-7.70 (m, 3H), 7.64-7.62 (d, 2H), 7.54-7.37 (m, 2H), 7.36-7.34 (d, 1H), 6.75-6.73 (d, J=8Hz, 1H), 4.51-4.48 (s, J=12Hz, 2H), 3.83-3.80 (s, J=8Hz, 1H), 2.21 (s, 2H), 1.97 (s, 6H), 1.44-1.26 (m, 39H). ^{13}C NMR (100 MHz, $CDCl_3$) δ: 165.9,

153.2, 146.0, 144.3, 140.7, 140.1, 139.7, 139.4, 137.3, 136.3, 130.3, 129.3, 129.2,129.0, 127.9, 126.9, 126.3,126.2, 126.0, 123.0, 121.6, 120.7, 120.1, 119.0, 114.2, 109.9, 109.5, 41.1, 41.6, 40.2, 40.1, 31.8, 31.8, 29.7, 29.7, 29.6, 29.5, 29.3, 29.2, 28.5, 27.8, 27.1, 27.0, 26.9, 22.7, 22.6, 14.1, 14.1. HRMS (ES+): $C_{49}H_{59}N_4OSBr$ requires 832.3593, found 832.7045. IR (KBr, cm^{-1}): 3442.88, 2920.94, 2849.89, 1691.52, 1609.64, 1481.35, 1459.34, 1434.60, 1367.22, 1339.86, 1259.77.

Spectral data

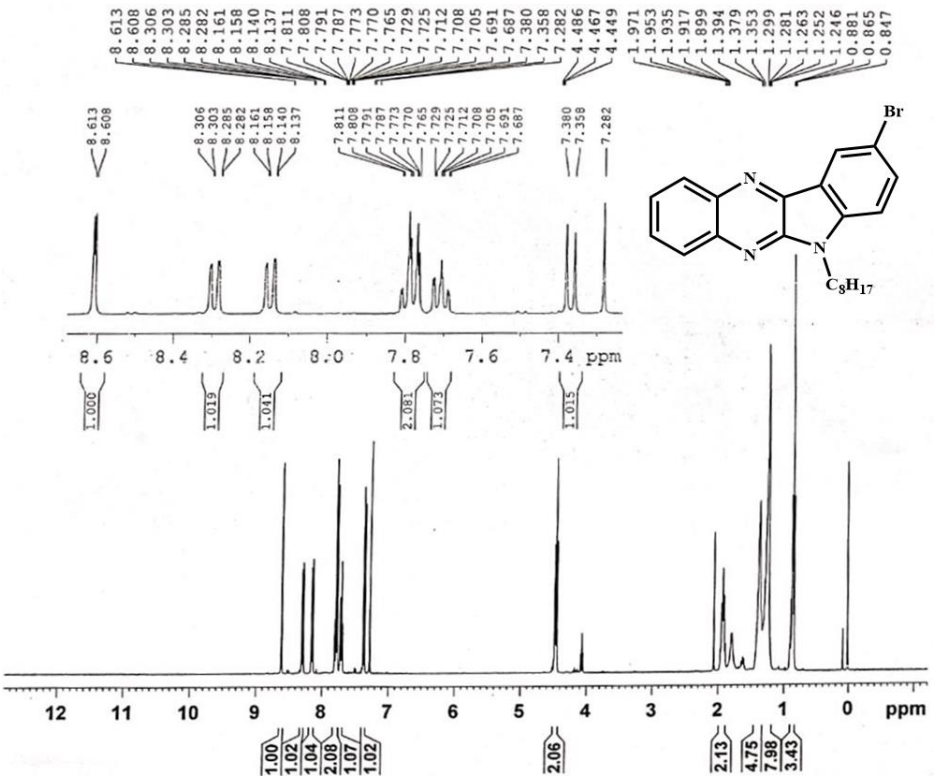

Figure 5.13 ^{1}H NMR of compound **2**

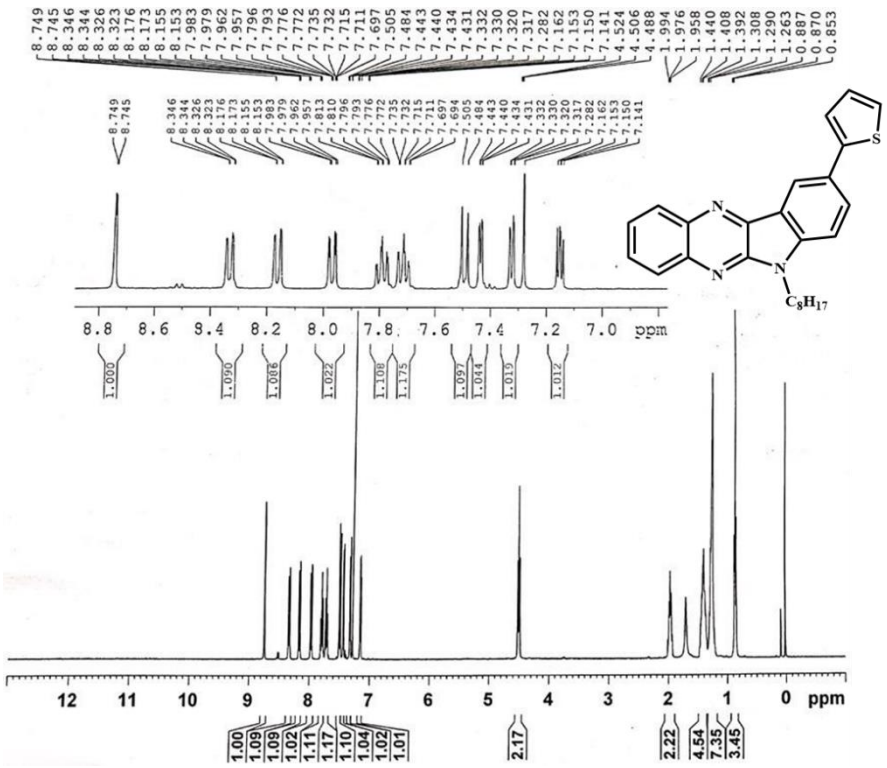

Figure 5.14 ^{1}H NMR of compound **3**

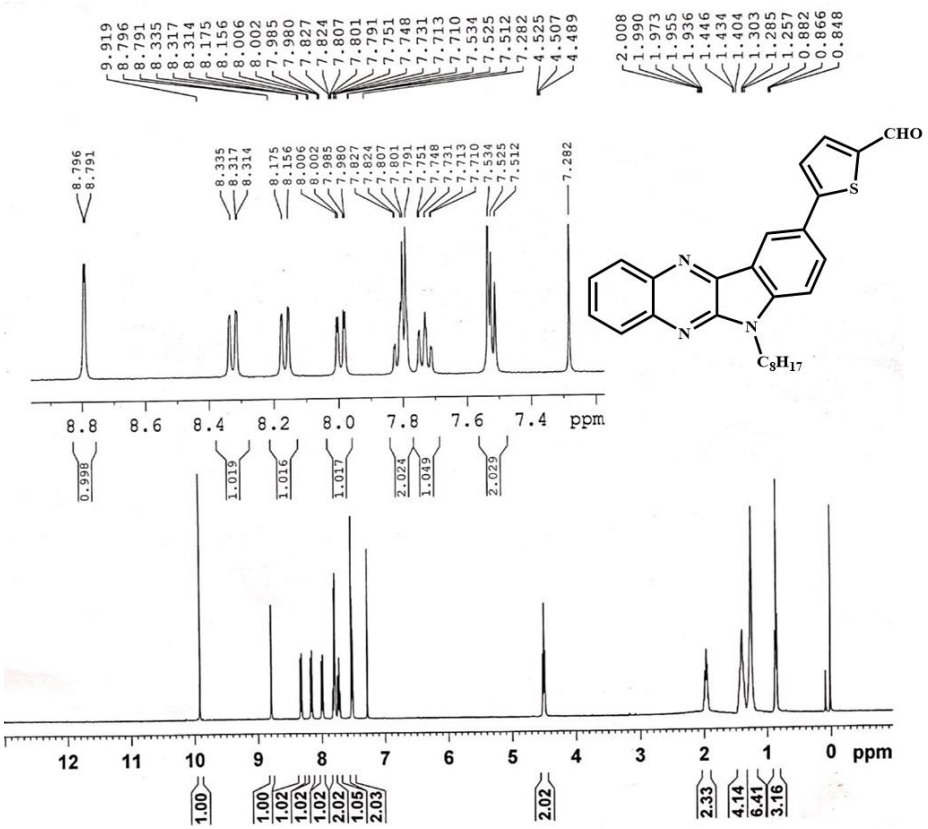

Figure 5.15 ^{1}H NMR of compound **4**

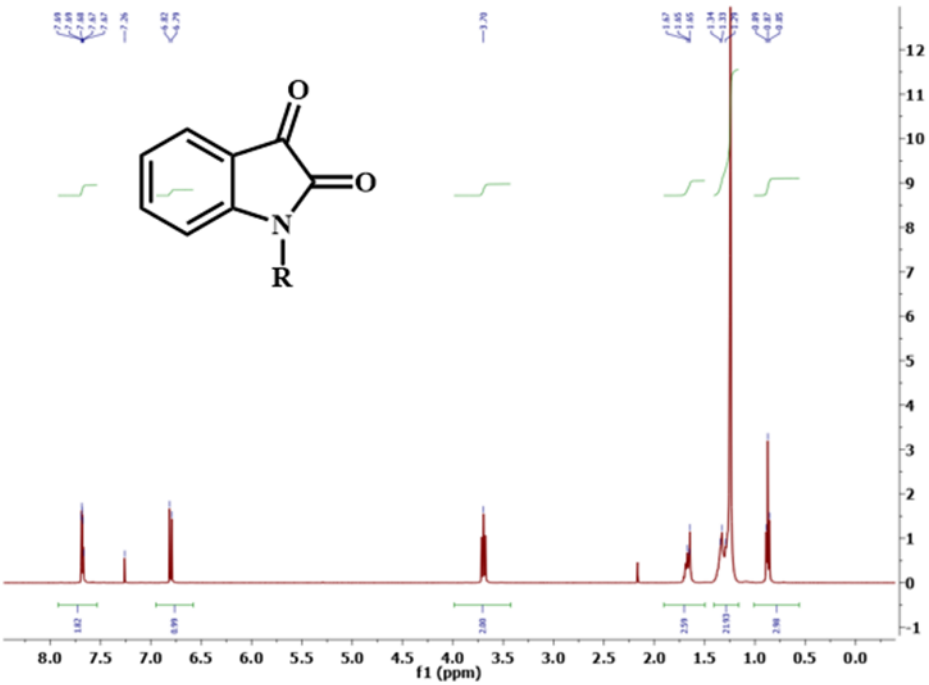

Figure 5.16 ^{1}H NMR of compound **5**

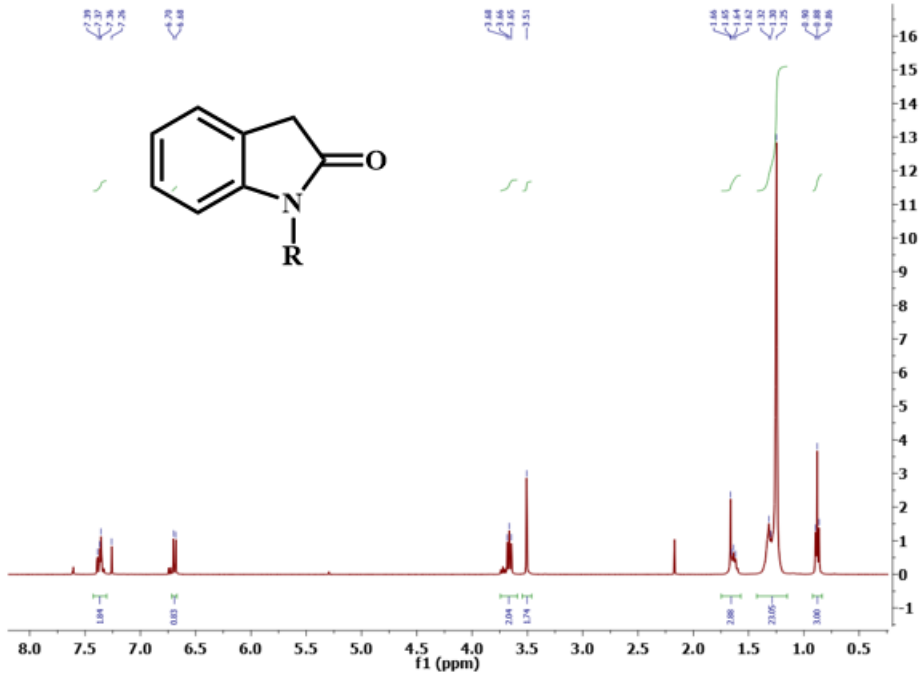

Figure 5.17 ^{1}H NMR of compound **6**

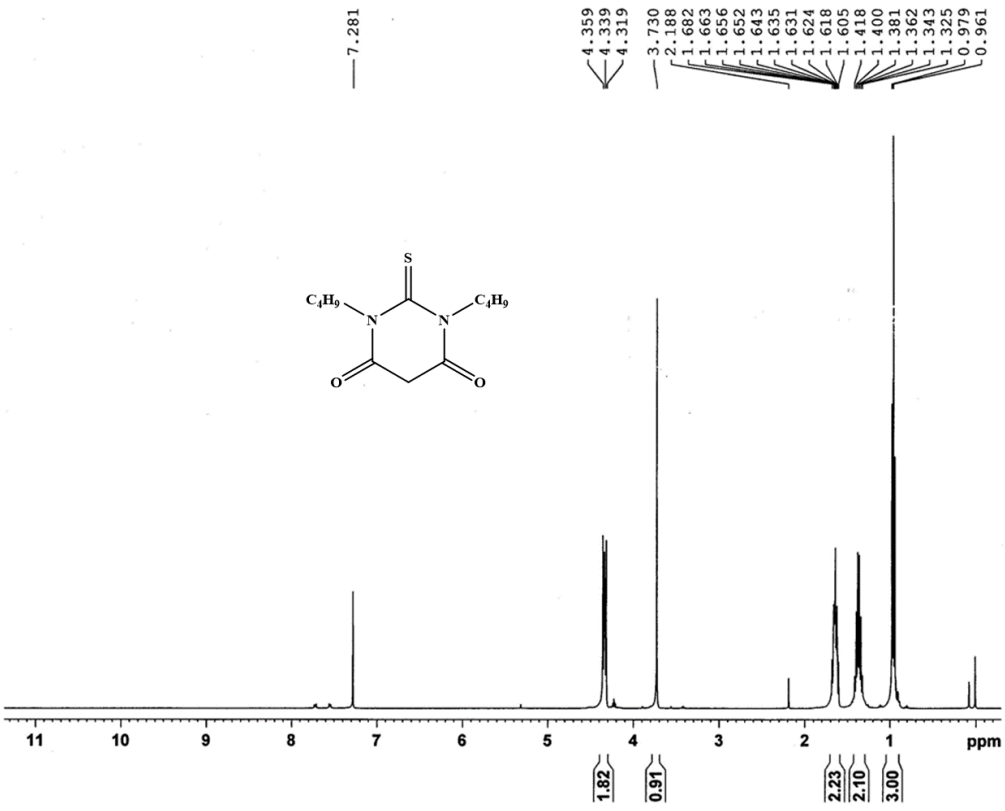

Figure 5.18 ^{1}H NMR of compound **7**

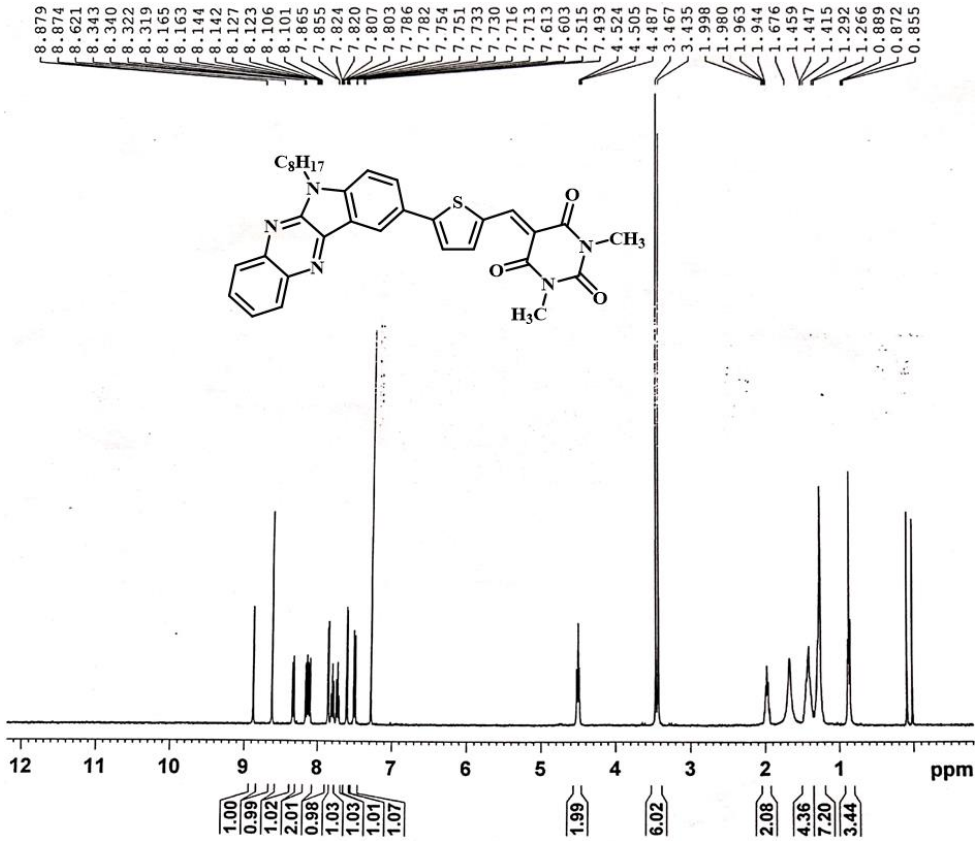

Figure 5.19 ^{1}H NMR of compound **IIQXN-BA**

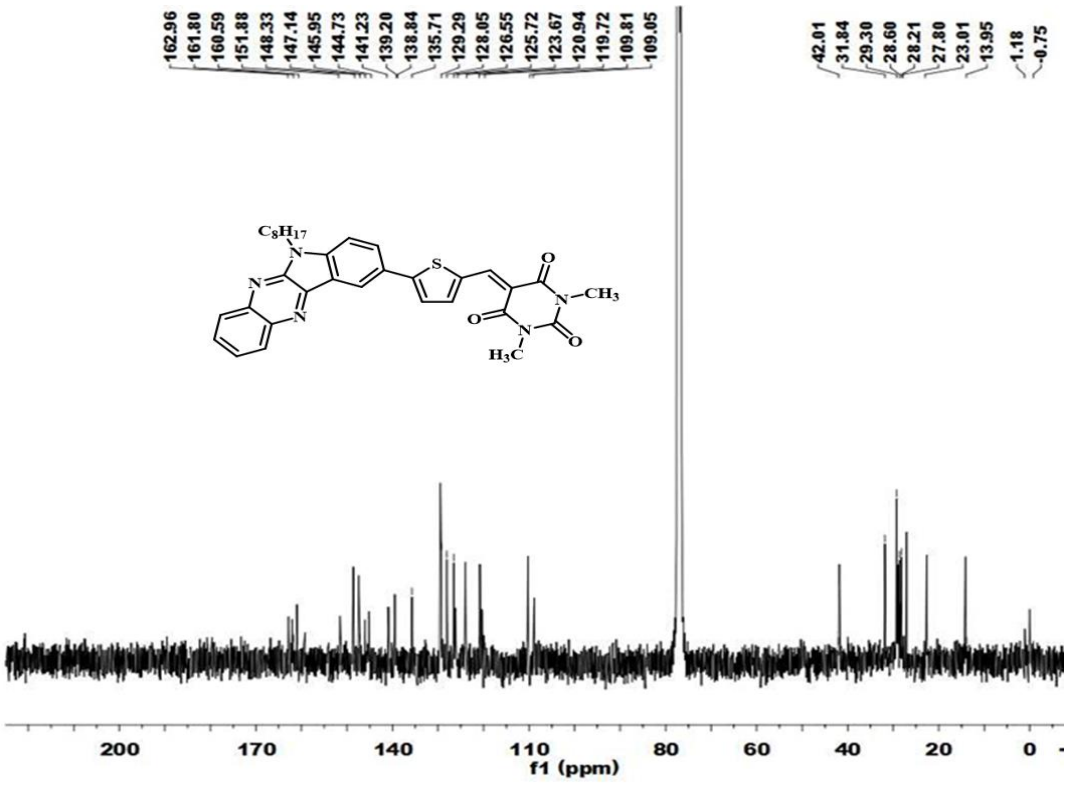

Figure 5.20 ^{13}C NMR of compound **IIQXN-BA**

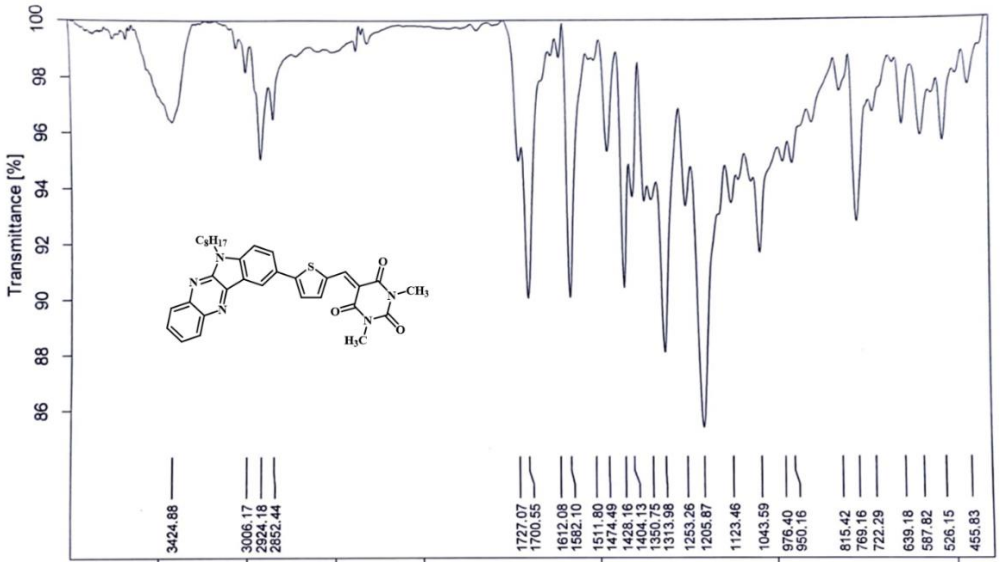

Figure 5.21 IR data of compound **IIQXN-BA**

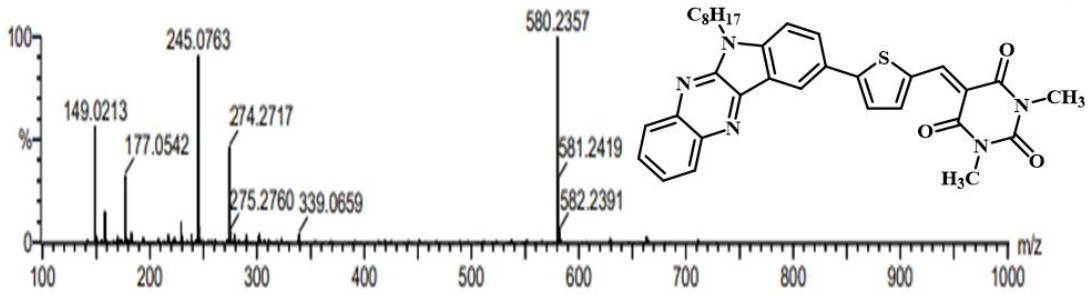

Figure 5.22 HRMS data of compound **IIQXN-BA**

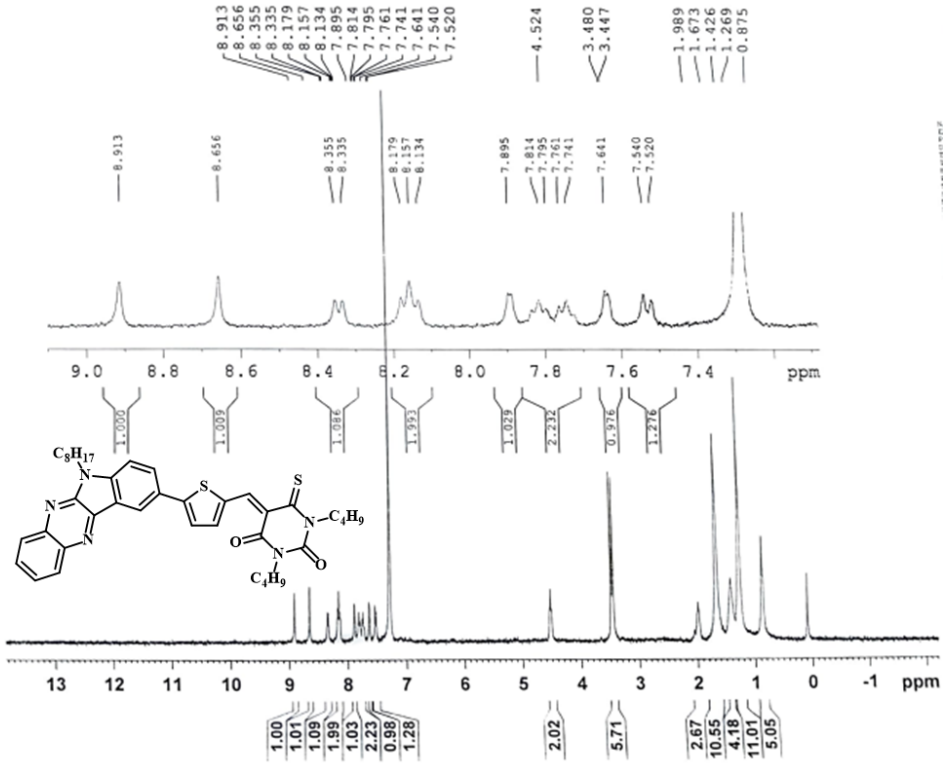

Figure 5.23 ^{1}H NMR of compound **IIQXN-TBA**

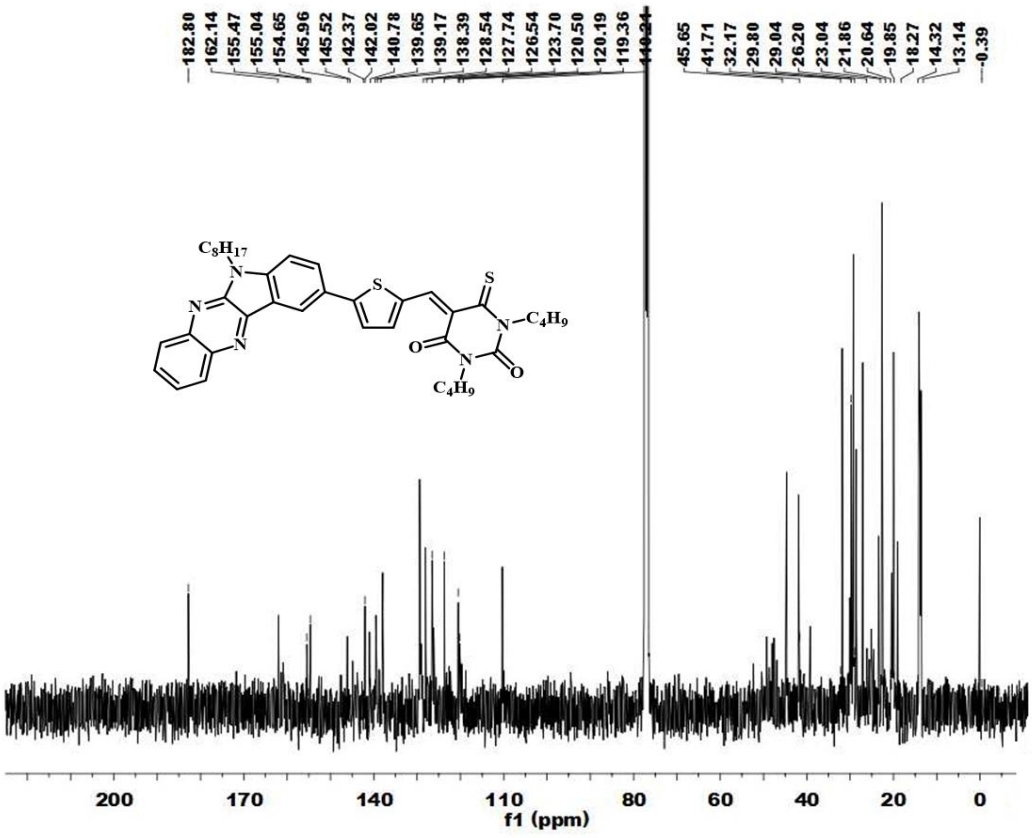

Figure 5.24 ^{13}C NMR of compound **IIQXN-TBA**

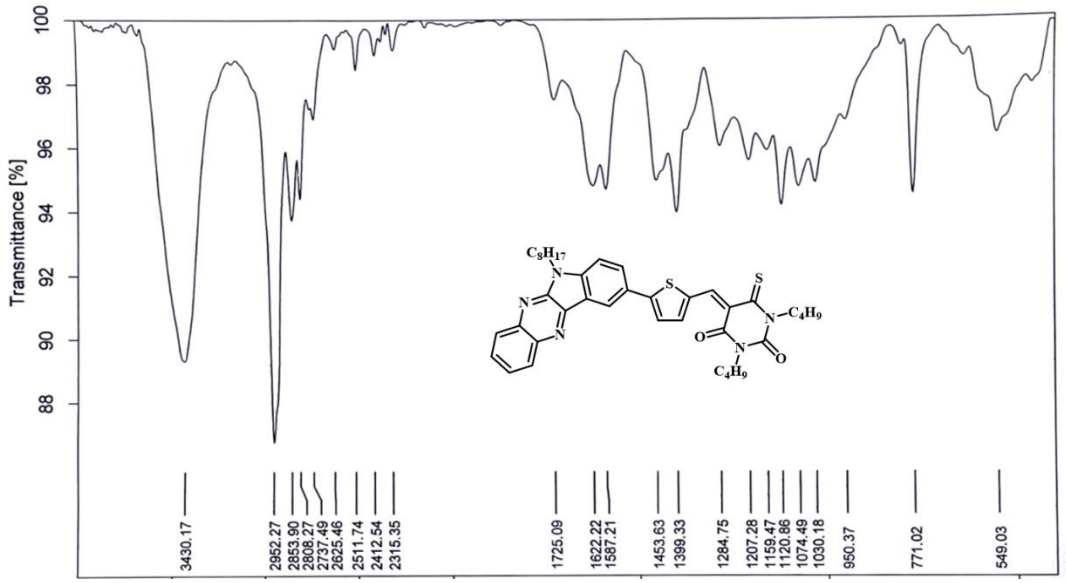

Figure 5.25 IR data of compound **IIQXN-TBA**

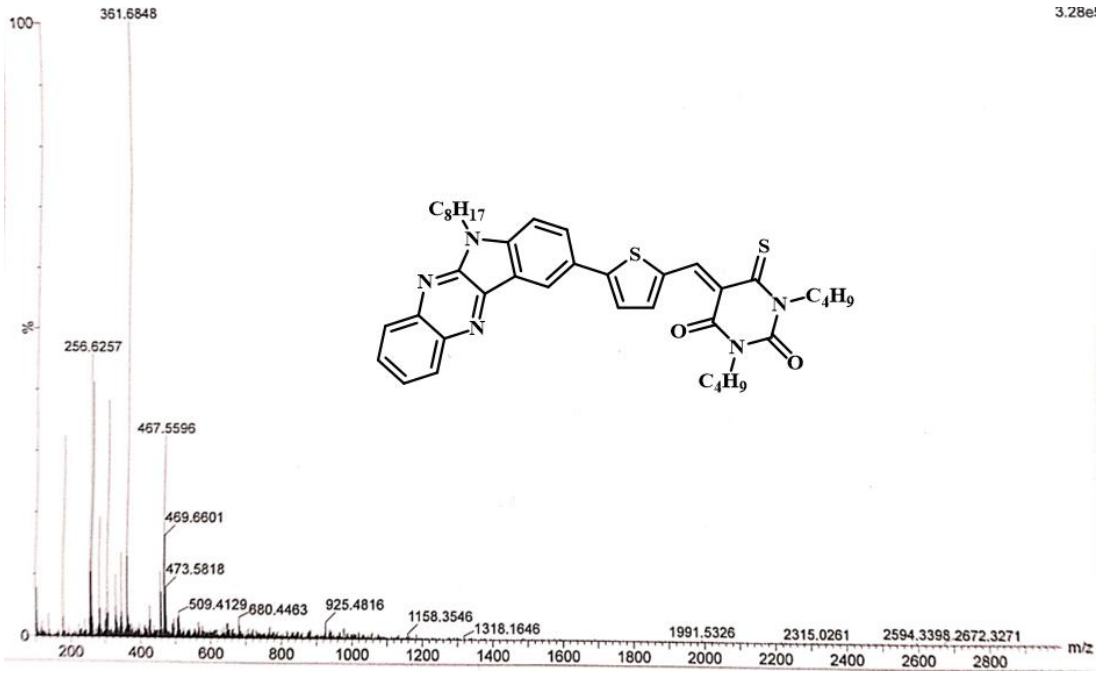

Figure 5.26 HRMS data of compound **IIQXN-TBA**

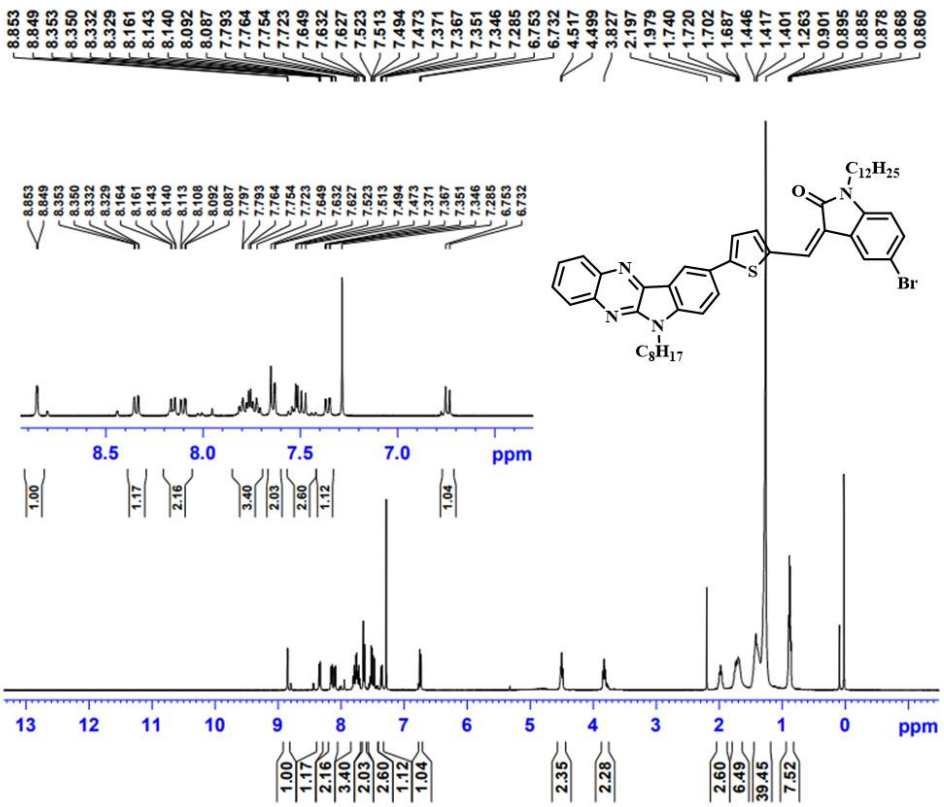

Figure 5.27 ^{1}H NMR of compound **IIQXN-RI**

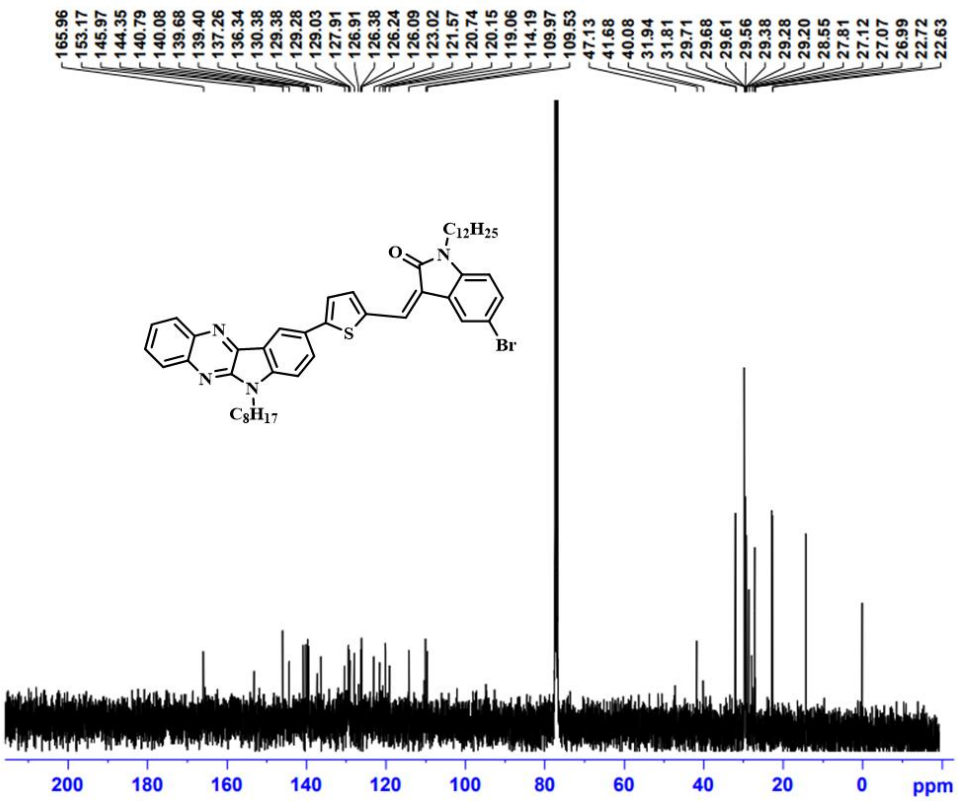

Figure 5.28 ^{13}C NMR of compound **IIQXN-RI**

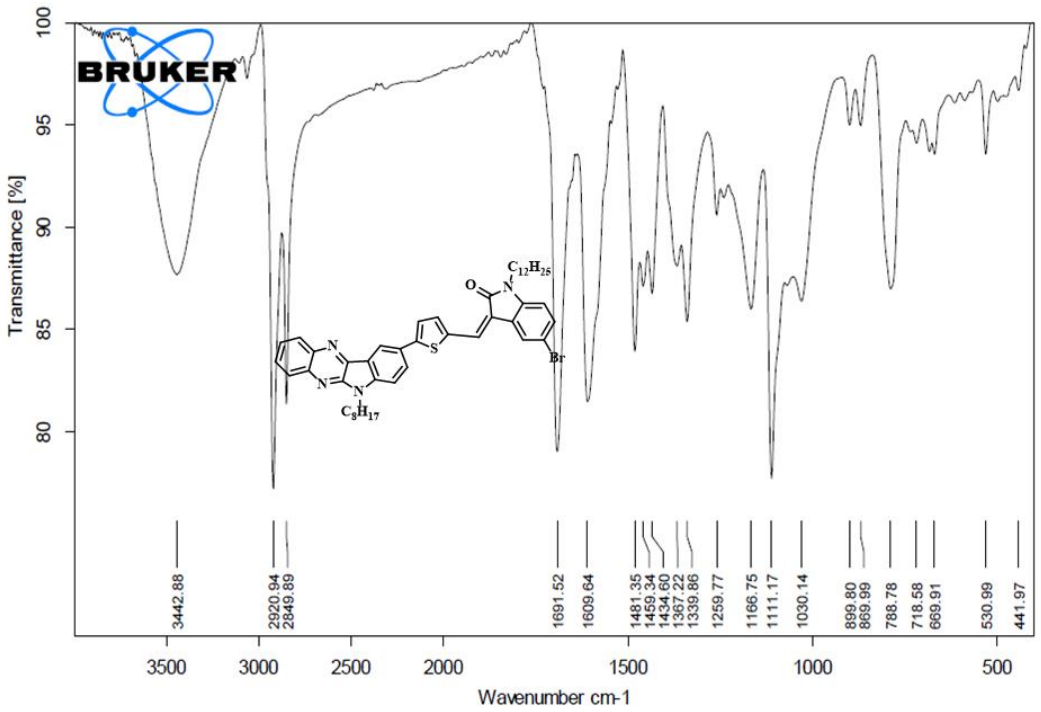

Figure 5.29 IR data of compound **IIQXN-RI**

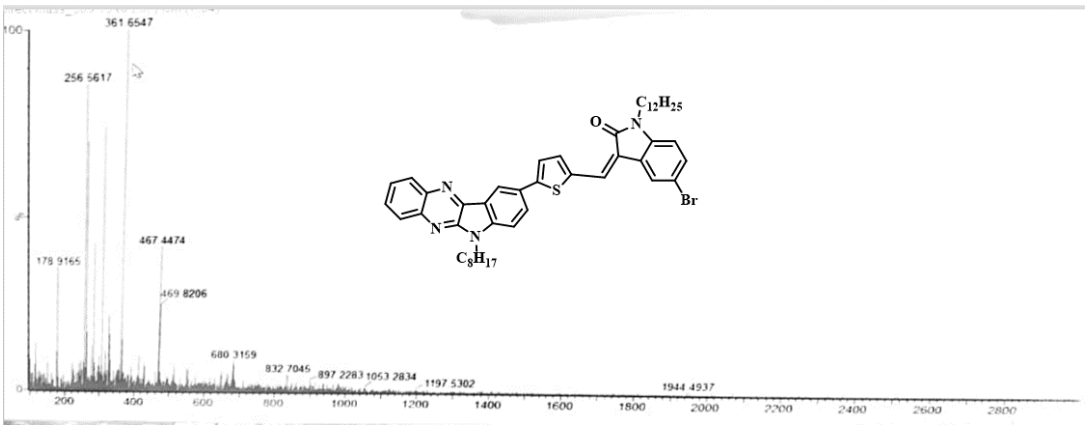

Figure 5.30 HRMS data of compound **IIQXN-RI**

References

1 M. M. Zhang, Y. H. Ma, P. Li, Y. Jia and K. L. Han, *Chem. Commun.*, 2020, **56**, 2610–2613.

2 Q. Hu, C. Qin, L. Huang, H. Wang, Q. Liu and L. Zeng, *Dye. Pigment.*, 2018, **149**, 253–260.

3 J. S. Lan, L. Liu, R. F. Zeng, Y. H. Qin, Y. Liu, X. Y. Jiang, A. Aihemaiti, Y. Ding, T. Zhang and R. J. Y. Ho, *Chem. Commun.*, 2020, **56**, 1219–1222.

4 Z. Zhou, J. Gu, X. Qiao, H. Wu, H. Fu, L. Wang, H. Li and L. Ma, *Sensors Actuators, B Chem.*, 2019, **282**, 437–442.

5 N. Altinolcek, A. Battal, C. N. Vardalli, M. Tavasli, H. A. Yu, W. J. Peveler and P. J. Skabara, *J. Mol. Struct.*,2021, 16, 1066-1074. .

6 H. Li, F. S. Kim, G. Ren and S. A. Jenekhe, *J. Am. Chem. Soc.*, 2013, **135**, 14920–14923.

7 J. Lv, Y. Chen, F. Wang, T. Wei, Z. Zhang, J. Qiang and X. Chen, *Dye. Pigment.*, 2018, **148**, 353–358.

8 V. Pirovano, M. Marchetti, J. Carbonaro, E. Brambilla, E. Rossi, L. Ronda and G. Abbiati, *Dye. Pigment.*, 2020, **173**, 107917-107930.

9 B. Zhang, H. Wu, Z. Wang, A. Qin and B. Z. Tang, *J. Mater. Chem. C*, 2020, **8**, 4754–4762.

10 H. Yan, X. Meng, B. Li, S. Ge and Y. Lu, *J. Mater. Chem. C*, 2017, **5**, 10589–10599.

11 P. Ledwon, *Org. Electron.*, 2019, **75**, 105422-105437.

12 J.-L. Li, Y.-F. Chai, W. V. Wang, Z.-F. Shi, Z.-G. Xu and H.-L. Zhang, *Chem. Commun.*, 2017, **53**, 5882–5885.

13 P. Thongkasee, A. Thangthong, N. Janthasing, T. Sudyoadsuk, S. Namuangruk, T. Keawin, S. Jungsuttiwong and V. Promarak, *ACS Appl. Mater. Interfaces*, 2014, **6**, 8212–8222.

14 X. Qian, Y. Z. Zhu, W. Y. Chang, J. Song, B. Pan, L. Lu, H. H. Gao and J. Y.

Zheng, *ACS Appl. Mater. Interfaces*, 2015, **7**, 9015–9022.

15 Y. Ooyama, Y. Shimada, S. Inoue, T. Nagano, Y. Fujikawa, K. Komaguchi, I. Imae and Y. Harima, *New J. Chem.*, 2011, **35**, 111–118.

16 M. Meier, L. Ji, J. Nitsch, I. Krummenacher, A. Deißenberger, D. Auerhammer, M. Schäfer, T. B. Marder and H. Braunschweig, *Chem. - A Eur. J.*, 2019, **25**, 4707–4712.

17 S. Tsumura, T. Enoki and Y. Ooyama, *Chem. Commun.*, 2018, **54**, 10144–10147.

18 K. Starzak, A. Matwijczuk, B. Creaven, A. Matwijczuk, S. Wybraniec and D. Karcz, *Int. J. Mol. Sci.*, 2019, **20**, 1–17.

19 Y. Jiang, Y. Gao, H. Tian, J. Ding, D. Yan, Y. Geng and F. Wang, *Macromolecules*, 2016, **49**, 2135–2144.

20 A. Abbotto, L. Beverina, R. Bozio, A. Facchetti, C. Ferrante, G. A. Pagani, D. Pedron and R. Signorini, *Chem. Commun.*, 2003, **3**, 2144–2145.

21 N. Altinolcek, A. Battal, C. N. Vardalli, M. Tavasli, H. A. Yu, W. J. Peveler and P. J. Skabara, *J. Mol. Struct.*, 2021, **1239**, 130494-130503.

22 W. Sun, G. Hu, W. Shen, H. Xu, Z. Deng, G. Zhao, F. Li, Y. Hu and W. Yang, *J. Mol. Liq.*, 2021, **340**, 116846.

23 X. Zhang, F. Zhang, B. Yang and B. Liu, *Spectrochim. Acta - Part A Mol. Biomol. Spectrosc.*, 2021, **258**, 119827-119836.

24 Y. Wang, H. Wu, W. N. Wu, S. J. Li, Z. H. Xu, Z. Q. Xu, Y. C. Fan, X. L. Zhao and B. Z. Liu, *Sensors Actuators, B Chem.*, 2018, **260**, 106–115.

25 J. T. Hou, H. S. Kim, C. Duan, M. S. Ji, S. Wang, L. Zeng, W. X. Ren and J. S. Kim, *Chem. Commun.*, 2019, **55**, 2533–2536.

26 B. Liu, J. Wang, G. Zhang, R. Bai and Y. Pang, *ACS Appl. Mater. Interfaces*, 2014, **6**, 4402–4407.

27 X. Qian, X. Wang, L. Shao, H. Li, R. Yan and L. Hou, *J. Power Sources*, 2016, **326**, 129–136.

28 A. Arunkumar, M. Deepana, S. Shanavas, R. Acevedo and P. M. Anbarasan,

ChemistrySelect, 2019, **4**, 4097–4104.

29 A. Mahmood, *Sol. Energy*, 2016, **123**, 127–144.

30 K. Zeng, Z. Tong, L. Ma, W. H. Zhu, W. Wu, Y. Xie and Y. Xie, *Energy Environ. Sci.*, 2020, **13**, 1617–1657.

31 R. Sánchez-De-Armas, M. Á. San Miguel, J. Oviedo and J. F. Sanz, *Phys. Chem. Chem. Phys.*, 2012, **14**, 225–233.

32 Z. Li, C. C. Chueh and A. K. Y. Jen, *Prog. Polym. Sci.*, 2020, **179**, 108419.

33 K. R. J. Thomas and P. Tyagi, *J. Org. Chem.*, 2010, **75**, 8100–8111.

34 J. Ren, P. Zhang, H. Liu, C. Zhang, Y. Gao, J. Cui and J. Chen, *Sensors Actuators, B Chem.*, 2020, **304**, 127299.

35 X. Li, J. Gu, H. Huang, Z. Zhou, J. Gao and Q. Wang, *Dye. Pigment.*, 2020, **181**, 108545.

36 H. Masui, M. M. Maitani, S. Fuse, A. Yamamura, Y. Ogomi, S. Hayase, T. Kaiho, H. Tanaka, Y. Wada and T. Takahashi, *Asian J. Org. Chem.*, 2018, **7**, 458–464.

37 T. Xu and L. Yu, *Mater. Today*, 2014, **17**, 11–15.

38 S. Fuse, M. Takizawa, K. Matsumura, S. Sato, S. Okazaki and H. Nakamura, *European J. Org. Chem.*, 2017, **2017**, 5170–5177.

39 Z. Li, Y. Pei, S. Hou, Y. Dai, D. Liu, J. Zhu, Y. P. Zhu and X. Liu, *Dye. Pigment.*, 2020, **179**, 108419-108427.

40 V. J. Bhanvadia, A. Choudhury, P. K. Iyer, S. S. Zade and A. L. Patel, *Polymer (Guildf).*, 2020, **210**, 123032.

41 P. Tyagi, A. Venkateswararao and K. R. J. Thomas, *J. Org. Chem.*, 2011, **76**, 4571–4581.

42 H. Wu, Y. Chen, X. Ling, W. Yuan, B. Li and Z. Zhou, *J. Mol. Liq.*, 2021, **329**, 115465.

43 A. J. Payne, J. S. J. McCahill and G. C. Welch, *Dye. Pigment.*, 2015, **123**, 139–146.

44 M. Jha, G. M. Shelke and A. Kumar, *European J. Org. Chem.*, 2014, **2014**, 3334–3336.

45 V. Chahal, S. NIRWAN and R. Kakkar, *Med. Chem. Commun.*, 2019, **10**, 351-368..

46 Z. Tribak, A. Haoudi, Y. Kandri Rodi, H. Elmsellem, M. K. Skalli, Y. Ouzidan, A. Mazzah and E. Essassi, *Moroccan J. Chem Mor. J. Chem*, 2016, **4**, 1157–1163.

47 M. Klikar, V. Jelínková, Z. Růžičková, T. Mikysek, O. Pytela, M. Ludwig and F. Bureš, *European J. Org. Chem.*, 2017, **2017**, 2764–2779.

48 N. Shalini and R. Sarah, *Appl. Spectrosc.*, 2001, **55**, 362A-370A.

49 A. Venkateswararao, P. Tyagi, K. R. Justin Thomas, P. W. Chen and K. C. Ho, *Tetrahedron*, 2014, **70**, 6318–6327.